COSMOGONY OF THE SOLAR SYSTEM

G. P. HOREDT

Max Planck Institut für Astrophysik, München, Germany

Abstract. In Sections 1–6, we determine an approximate analytical model for the density and temperature distribution in the protoplanetary cloud. The rotation of the planets is discussed in Section 7 and we conclude that it cannot be determined from simple energy conservation laws.

The velocity of the gas of the protoplanetary cloud is found to be smaller by about 5×10^3 cm s^{-1} in comparison to the Keplerian circular velocity. If the radius of the planetesimals is smaller than a certain limit r_1, they move together with the gas. Their vertical and horizontal motion for this case is studied in Sections 8 and 9.

As the planetesimals grow by accretion their radius becomes larger than r_1 and they move in Keplerian orbits. As long as their radius is between r_1 and a certain limit r_2 their gravitational interaction is negligible. In Section 10, we study the accretion for this case.

In Section 11, we determine the change of the relative velocities due to close gravitational encounters. The principal equations governing the late stages of accretion are deduced in Section 12. In Section 13 there are obtained approximate analytical solutions.

The effect of gas drag and of collisions is studied in Sections 14 and 15, respectively. Numerical results and conclusions concerning the last and principal stage of accretion are drawn in Section 16.

1. Simplifying Assumptions

We assume that around the Sun there revolves in circular orbit the protoplanetary cloud of gas and dust, which is prevented by its large angular momentum from infall. The protoplanetary cloud possesses a strong density concentration towards its equatorial plane, (e.g., Safronov, 1969; Kusaka *et al.*, 1970; Cameron, 1973; and our Section 4).

Below we give some justification for having neglected magnetic fields, turbulence and gravitational instability. A first general justification is the fact that we are able to model the formation of the planets without these three phenomena. A second point is that their occurrence is questionable.

(i) *Magnetic Fields.* At present there exists no convincing evidence that magnetic fields have played a decisive role in the formation history of the planetary system excepting perhaps the resolution of the angular momentum problem of the collapsing Sun (Okamoto, 1969; Horedt, 1978b) and the slowing down of a fast spin rate of the primordial Sun (Mestel, 1970). Because of the transient nature of magnetic fields and the high degree of arbitrariness concerning strength and structure of the fields we have neglected magnetic fields.

(ii) *Turbulence.* A necessary but not sufficient condition for the onset of turbulence is that $Re \gtrsim 10^6$ (ter Haar, 1972; Horedt, 1975b), where Re denotes the Reynolds number. The Reynolds number depends on two somewhat arbitrary numbers, the characteristic length and the characteristic velocity and could be made for the protoplanetary

cloud equal to about 10^{11} (Safronov, 1969; ter Haar, 1972). But the nonrandom orientation of the spin axes of stars in galactic clusters (Ferrer and Jaschek, 1973) as well as the tendency towards perpendicularity between spin axes of binaries and their orbital plane (Weis, 1974) show that turbulence does not play a decisive role, even during collapse of the Sun. Because turbulence, if it occurs at all, dissipates during several years in the protoplanetary cloud (Safronov, 1969; ter Haar, 1972), we have it neglected.

(iii) Most authors agree that the density of the protoplanetary cloud was too low for gravitational instability to occur, (e.g., Goldreich and Ward, 1973). Moreover, because of analytical difficulties, most authors establish merely the instability conditions in an idealized medium (Horedt, 1970; 1973b) without investigating the behaviour after onset of instability. Numerical work (Larson, 1972a; Black and Bodenheimer, 1976) on rotating collapsing clouds does not show concludent results with respect to the onset of instability in the protoplanetary cloud.

We have neglected also fragmentation of colliding planetesimals because it does not seem to be important at the low relative velocities occurring in our model (Figure 10). Besides, we have only uncertain information about the velocities of fragmented planetesimals and their mass distribution function (e.g., Bandermann, 1972; Hallam and Marcus, 1974; Kaula and Bigeleisen, 1975).

2. The Mass Excess in the Protoplanetary Cloud

The actual mass of the planetary system is about $0.0014M$ (M = solar mass) and it seems not likely that the mass of the protoplanetary cloud was larger than $0.1M$. Below, we summarize our arguments.

(i) The mass of the protoplanetary cloud deduced from the actual mass of the planetary system and corrected for additional gas content should be larger than $0.01M$ and lower than about $0.07M$, (Weidenschilling, 1977b, and our Section 5).

(ii) A mass excess of the protoplanetary cloud considerably larger than $0.1M$ poses the question where this additional mass has gone. We are not able to show what could happen with about 10–100 Earth masses of rocky planetesimals spread in the region of the terrestrial planets. Why there exist at present only remnants of about 2 Earth masses with bodies as small as the asteroids? The large amount of gas could be blown away by an intense T-Tauri-like solar wind, (Horedt, 1978a). However, according to Bodenheimer, (1972; p. 18) it seems unlikely that an ordinary star loses more than a negligible fraction of its mass during the T-Tauri stage, mainly because the mass loss rates deduced initially by Kuhi seem to be grossly overestimated. It seems therefore very difficult to understand how the T-Tauri-like solar wind with a total mass of only several percent of solar mass could blow away from the protoplanetary cloud gases with mass exceeding considerably its own mass. To be on the safe side, we use throughout for the protoplanetary cloud its minimum mass of $0.011M$ from Section 5.

3. The Temperature Problem in the Protoplanetary Cloud

From the theoretical viewpoint, grains could be melted completely even at Pluto's distance from the Sun by a contracting gas sphere in quasihydrostatic equilibrium, as will be shown subsequently. We identify the contracting gas sphere with the Sun.

(i) For convective equilibrium of the outer parts of a gaseous sphere we can integrate immediately the equation of hydrostatic equilibrium

$$dp/dr = -GM\rho/R^2, \tag{3.1}$$

where p and ρ is the pressure and density of the gas, G the gravitational constant, M is the solar mass (a constant) and R is the distance from the Sun. The adiabatic equation of state is valid: $p = \text{const } \rho^\gamma$, where γ is the ratio between the specific heats at constant pressure and volume. Equation (3.1) yields

$$T - T_0 = (\gamma - 1)\mu GM(1/R - 1/R_0)/\mathscr{R}\gamma, \tag{3.2}$$

where we have used the ideal gas law

$$p = \mathscr{R}\rho T/\mu, \tag{3.3}$$

where T is the temperature of the gas, $\mathscr{R}$ the gas constant and $\mu = 2.4$ (Kusaka et al., 1970) the mean molecular weight of the gas of the protoplanetary cloud. The radiation pressure $a_s T^4/3$ (a_s is the Stefan constant) is neglected throughout with respect to the gas pressure from Equation (3.3)–i.e.,

$$\rho \gg \mu a_s T^3/3\mathscr{R}. \tag{3.4}$$

(ii) For radiative equilibrium of the outer parts we have to add to Equation (3.1) the equation of radiative equilibrium

$$dT/dR = -3\kappa L\rho/16\pi a_s cR^2 T^3, \tag{3.5}$$

and solve simultaneously. c denotes the velocity of light, L is the luminosity of the Sun (a constant) and $\kappa = \kappa_0 p^\alpha T^\beta$ the opacity (κ_0, α, $\beta = \text{const.}; \alpha \neq -1; \beta \neq 4$). Dividing Equation (3.1) by (3.5) we obtain with the boundary condition $p = 0$ if $T = 0$ the equation

$$(\mathscr{R}/\mu)^{\alpha+1}\rho^{\alpha+1}/(\alpha + 1) = 16\pi a_s cGMT^{3-\beta-\alpha}/3(4 - \beta)L\kappa_0.$$

Inserting into Equation (3.5) and integrating we obtain an equation similar to Equation (3.2), (cf. Chandrasekhar (1939) for Kramers opacity)

$$T - T_0 = (\alpha + 1)\mu GM((1/R) - (1/R_0))/(4 - \beta)\mathscr{R}. \tag{3.6}$$

Assuming that $T_0 \approx 0$ if $R_0 \gg R$, we have from Equations (3.2) and (3.6)

$$T \approx \mu GM/\mathscr{R}R = 3.8 \times 10^{18}/R;$$

i.e. $T \approx 6500$ K for Pluto.

It should be noted that, because of rapid gravitational contraction, such a high

TABLE I

Temperature of the planetesimals near the equatorial plane of the protoplanetary cloud. T_{chem} is from Lewis (1972, 1974)

Planet	AU	T_{chem}	$T(L_\odot)$	$T(81L_\odot)$	T_b	T_{be}
Mercury	0.4	1400 K	442 K	1326 K	172 K	139 K
Venus	0.7	900	325	975	122	99
Earth	1.0	600	276	828	103	83
Mars	1.5	450	224	672	84	68
Asteroids	2.8	300	165	495	64	52
Jupiter (satellites)	5.2	150	121	363	49	40
Saturn (satellites)	9.5	100	89	267	37	30
Uranus	19.3	75	63	189	28	23
Neptune	30.2	50	50	150	24	19
Pluto	39.8	–	44	132	22	18

temperature could last only for an interval $t = (R^3/2GM)^{1/2}$, (2 years for Pluto), of the order of the free fall time (Larson, 1972a; Cameron, 1973; Horedt, 1976).

The temperature distribution near the equatorial plane of the protoplanetary cloud as inferred from chemical studies of meteorites and the composition of the planets and satellites is shown in the first column of Table I and seems the most reliable one (Anders, 1972; Lewis, 1974). It corresponds approximately to a temperature distribution

$$T_{\text{chem}} \propto 1/R. \tag{3.7}$$

Even if we assume that the chemical composition of the planets is already fixed by meter-sized planetesimals, the temperature T_{chem} should be maintained for at least 10^3 yr in the inner parts of the solar system and for 10^5 yr in the outer parts (see Table III).

We have already shown that during gravitational contraction of the Sun extending up to Pluto's orbit, high temperatures ($T \gtrsim 1000$ K) could be maintained in the protoplanetary cloud only for several years. If we assume a supermassive ($1M$) protoplanetary cloud, then a temperature of order T_{chem} could be maintained for about 10^3 yr by gravitational energy liberated from contraction of this cloud (Cameron and Pine, 1973, Fig. 14; Cameron, 1973). However, as it is obvious from Section 2 such a high mass of the protoplanetary cloud introduces other difficulties.

In the following, a possibility of attaining a temperature comparable to T_{chem} by a simple radiation controlled temperature distribution is indicated.

The temperature estimate from Equation (3.7) is valid with some approximation only for the planetesimals of the protoplanetary cloud. The temperature of the gas of the protoplanetary cloud could differ grossly from the temperatures used in this paper (see Section 5), though we have assumed for simplicity that gas and planetesimals have approximately the same temperature.

We distinguish two different stages in the evolution of the protoplanetary cloud,

namely when the cloud is opaque to solar radiation and when it is approximately transparent (Section 5).

If the protoplanetary cloud is opaque to solar radiation, only its surface will be heated by the Sun up to temperatures T_b shown in Table I according to Equation (5.3) for a luminosity L of the Sun equal to its actual luminosity $L_\odot$. The last column shows the temperature T_{be} that would appear in the equatorial plane of the opaque protoplanetary cloud calculated from Equation (5.5). It will be argued in Section 5 that the opaque stage of the protoplanetary cloud is not likely to last for long time.

If the protoplanetary cloud is transparent to solar radiation, the temperature of a spinning planetesimal is given approximately by the black body temperature at distance R, (e.g., Larson, 1972b)

$$T = (L/4a_s cR^2)^{1/4}. \tag{3.8}$$

Table I shows T from Equation (3.8) for $L = L_\odot$ and $L = 81L_\odot$. With respect to the possibility of a high luminosity phase of the Sun we refer to the calculations of Larson (1972a), which show that the Sun could reach a maximum luminosity of $25L_\odot$ for about 10^5 yr. A luminosity of about $100L_\odot$ is also reconcilable with hydrodynamic calculations but only for about 10^4 yr (Kusaka et al., 1970; Fig. 1; Bodenheimer, 1972; Fig. 6).

T_{chem} from Table I is included between the values of T for $L = L_\odot$ and $L = 81L_\odot$. From Table VI, it appears that the accretion time of a planet increases with increasing distance from the Sun by about four orders of magnitude. T_{chem} is in agreement with the temperature T from Equation (3.8) if we assume a continuous decrease of solar luminosity from about $100L_\odot$ during the formation of the terrestrial planets to its present value $L_\odot$ during the formation of the outer planets.

For a given constant luminosity of the Sun we have near the equatorial plane of the cloud (see Equations (3.7), (3.8), (5.4), (5.5))

$$T_{chem} \propto R^{-1}; \; T_b, T_{be} \propto R^{-3/7}; \; T \propto R^{-1/2}. \tag{3.9}$$

To sum up: during the earliest stages of contraction of the Sun and of the protoplanetary cloud grains (small planetesimals) could vaporize. Then, the temperature of the protoplanetary cloud falls rapidly (Anders, 1972, pp. 196–201) but is maintained at level T_{chem} by a high luminosity of the Sun, which decreases during accretion of the planets from about $100L_\odot$ to $L_\odot$.

4. Hydrostatic Model of the Protoplanetary Cloud

We can derive a self-consistent solution of the equations of hydrostatic equilibrium (Weizsäcker, 1943)

$$\partial p/\partial l = -GM\rho l/R^3 + \omega^2 l\rho,$$
$$\partial p/\partial z = -GM\rho z/R^3, \tag{4.1}$$

by assuming that the temperature changes as

$$T = AR^{-b}, \quad (A, b = \text{const.}; b > 0; b \neq 1) \tag{4.2}$$

l and z are cylindrical coordinates of a frame with the centre in the Sun. We have $R = (l^2 + z^2)^{1/2}$, where l is the distance from the rotation axis Oz, and z the height above the equatorial plane. ω is the angular velocity of the gas of the protoplanetary cloud, rotating circularly around the Sun. We follow closely Weizsäcker's (1943) solution of Equations (4.1) by introducing Equations (3.3), (4.2) into Equation (4.1) and making the substitution

$$\rho = \exp \varphi. \tag{4.3}$$

Equations (4.1) become

$$(\mathscr{R}AR^{-b}/\mu)(\partial\varphi/\partial l) - b\mathscr{R}AR^{-b-2}l/\mu = -GMl/R^3 + \omega^2 l, \tag{4.4}$$

$$(\mathscr{R}AR^{-b}/\mu)(\partial\varphi/\partial z) - b\mathscr{R}AR^{-b-2}z/\mu = -GMz/R^3. \tag{4.5}$$

From $R^2 = l^2 + z^2$ we have

$$\partial\varphi/\partial z = (z/R)\partial\varphi/\partial R. \tag{4.6}$$

Equation (4.6) is introduced into Equation (4.5) and the result can be integrated

$$\varphi = \ln R^b - GM\mu R^{b-1}/A\mathscr{R}(b-1) + B(l), \tag{4.7}$$

where $B(l)$ is an unknown function of l. Equation (4.4), with Equation (4.7), becomes

$$dB(l)/dl = \partial B(l)/\partial l = \mu\omega^2 R^b l/\mathscr{R}A. \tag{4.8}$$

Equation (4.8) shows that ω^2 must be of the form

$$\omega^2 = \varphi_1(l)/R^b, \tag{4.9}$$

since B is a function of l only. As will be obvious later it is convenient to express ω^2 in terms of the circular Keplerian angular velocity $(GM/l^3)^{1/2}$. This can be done by writing ω^2 under the additive form

$$\omega^2 = (GM/l^{3-b} + \varphi_2(l))/R^b, \tag{4.10}$$

where $\varphi_2(l)$ is an unknown function of l. We have in the equatorial plane

$$\omega^2|_{z=0} = GM/l^3 + \varphi_2(l)/l^b.$$

Introducing Equation (4.10) into Equation (4.8), we find that

$$B(l) = \mu GM l^{b-1}/\mathscr{R}A + \psi(l), \tag{4.11}$$

where

$$d\psi/dl = \mu l\varphi_2/\mathscr{R}A. \tag{4.12}$$

We substitute Equations (4.11) and (4.12) into Equation (4.7) and then into Equation (4.3)

$$\rho = R^b \exp(GM\mu(l^{b-1} - R^{b-1})/\mathscr{R}A(b-1) + \psi). \tag{4.13}$$

If we take into account the fact that

$$R^{b-1} \simeq l^{b-1}(1 + (b-1)z^2/2l^2) \text{ if } z \lesssim l/3, \tag{4.14}$$

Equation (4.13) transforms into

$$\rho = l^b \exp(-GM\mu z^2/2\mathscr{R}Al^{3-b} + \psi), \quad (z \lesssim l/3), \tag{4.15}$$

We assume that a planet in the equatorial plane at distance l from the Sun has formed from the matter in a ring of width Δl. Denoting by m the mass of this ring, we find that

$$m = 4\pi l \Delta l \int_0^{z_b} \rho \, dz \simeq 4\pi l \Delta l \int_0^\infty \rho \, dz$$

$$= 4\pi \exp \psi l^{1+b} \Delta l \int_0^\infty \exp(-GM\mu z^2/2\mathscr{R}Al^{3-b}) \, dz$$

$$= (8\pi^3 \mathscr{R}A/GM\mu)^{1/2} l^{(5+b)/2} \exp \psi \Delta l; \tag{4.16}$$

z_b will be defined only in Equation (4.30), by using the result that the mass of the cloud above height z_b is negligible. We have

$$m \simeq 2\pi \sigma l \Delta l, \tag{4.17}$$

where σ denotes the surface density of the protoplanetary cloud. Since $\sigma \propto l^{-3/2}$ (Weidenschilling, 1977b) and $\Delta l \propto l$ (Equation (4.20), we have

$$m = \text{const.} \, l^{1/2} \tag{4.18}$$

and from Equation (4.16)

$$(\exp \psi) l^{2+b/2} \Delta l = \text{const.} \tag{4.19}$$

We make the plausible assumption that the rings from which successive planets have collected their mass are adjacent and that their boundary lies midway between successive planets. We denote by l_{i-1}, l_i, l_{i+1} the mean distance of successive planets. According to our assumption

$$\Delta l_i = (l_{i+1} + l_i)/2 - (l_i + l_{i-1})/2 = (l_{i+1} - l_{i-2})/2$$

$$= (l_i q - l_i/q)/2 = l_i(q^2 - 1)/2q$$

$$\text{i.e. } \Delta l_i \propto l_i. \tag{4.20}$$

We have used the observational fact that the distance between successive planets is given approximately by the Titius–Bode law, written (cf. Nieto, 1975; Horedt et al., 1977) as

$$l_{i+1} = q l_i = 1.73 l_i, \quad (q = \text{const.}). \tag{4.21}$$

Introducing Equation (4.20) into Equation (4.19) we find that

$$\exp \psi \propto l^{-3-b/2} \tag{4.22}$$

From Equation (4.12) we get

$$\varphi_2 = (\mathscr{R}A/\mu l)\,d\psi/dl = -(3 + b/2)\mathscr{R}A/\mu l^2,$$

and using Equation (4.10) we have

$$\begin{aligned}
\omega^2 &= GM/R^b l^{3-b} - (3 + b/2)\mathscr{R}A/R^b \mu l^2 \\
&\simeq GM/l^3 - (3 + b/2)\mathscr{R}A/\mu l^{2+b} - bGMz^2/2l^5 \\
&\simeq GM/l^3 - (3 + b/2)\mathscr{R}A/\mu l^{2+b} \\
&= GM/l^3 - 13\mathscr{R}A/4\mu l^{5/2}, \quad (z \lesssim l/3),
\end{aligned} \tag{4.23}$$

We put $b = \frac{1}{2}$ as follows from Equation (3.8). It can be easily shown that for our numerical model the second-order term in z^2 arising in Equation (4.23) from the expansion of $R^{-1/2}$ is negligible with respect to $13\mathscr{R}A/4\mu l^{5/2}$ if $z \lesssim l/3$.

The difference between the Keplerian circular velocity V_c and the velocity V_g of the rotating gas of the cloud is found from Equation (4.23) to be

$$\begin{aligned}
V_c - V_g &= (GM/R)^{1/2} - \omega l \\
&\simeq (GM/l)^{1/2}((3 + b/2)\mathscr{R}Al^{1-b}/2\mu GM + z^2(-1 + b)/4l^2) \\
&= 13\mathscr{R}A/8\mu(GM)^{1/2} - (GM)^{1/2}z^2/8l^{5/2} \\
&\simeq 13\mathscr{R}A/8\mu(GM)^{1/2} = 5.25 \times 10^3 \text{ cm s}^{-1}, \quad (b = \tfrac{1}{2}; z \lesssim l/3)
\end{aligned}$$

where we have used also Equation (3.8) with $\hspace{4cm}$ (4.24)

$$A = (L/4\pi a_s c)^{1/4}. \tag{4.25}$$

Equation (4.15) underlines the great importance of the small velocity difference $V_c - V_g$ which assures the outward decrease of density in the protoplanetary cloud. For the density, we obtain from Equation (4.15) with the initial conditions $\rho = \rho(l_0, 0)$ at $l = l_0$, $z = 0$ and with Equations (3.8), (4.2) and (4.22)

$$\begin{aligned}
\rho(l, z) &= \rho(l_0, 0)(l/l_0)^{-3+b/2} \exp\left(-GM\mu z^2/2\mathscr{R}Al^{3-b}\right) \\
&= \rho(l_0, 0)(l/l_0)^{-11/4} \exp\left(-GM\mu z^2/2\mathscr{R}Tl^3\right); \\
&\quad (T \simeq Al^{-b}, b = \tfrac{1}{2}, z \lesssim l/3).
\end{aligned} \tag{4.26}$$

In the equatorial plane

$$\begin{aligned}
\rho(l, 0) &= \rho(l_0, 0)(l/l_0)^{-3+b/2} \\
&= \rho(l_0, 0)(l/l_0)^{-11/4}, \quad (b = \tfrac{1}{2}; z \lesssim l/3),
\end{aligned} \tag{4.27}$$

Inserting Equation (4.27) into Equation (4.26), we find for the density distribution with height (*cf.* Safronov, 1969) the expression

$$\rho(l, z) = \rho(l, 0) \exp\left(-GM\mu z^2/2\mathscr{R}Tl^3\right), \quad (z \lesssim l/3). \tag{4.28}$$

From Equation (4.28), we can determine a reasonable height z_b for the extension of the protoplanetary cloud. This could be given conveniently by the e-folding density

$$\rho(l, z_b)/\rho(l, 0) \; = \; 1/e \; = \; \text{const.} \tag{4.29}$$

With Equation (4.29), we obtain from Equation (4.28) the height

$$z_b \; = \; (2\mathscr{R}Tl^3/GM\mu)^{1/2}, \; (z_b \lesssim l/3), \tag{4.30}$$

Between the height $-z_b$ and z_b there is contained about 85% of the whole mass of the protoplanetary cloud. From the tables of the error function it results that the surface density σ_b between the heights $-z_b$ and z_b is related to the surface density σ between the heights $-\infty$ and ∞ by

$$\begin{aligned}
\sigma_b \; &= \; \int_{-z_b}^{z_b} \rho(l, z) \, \mathrm{d}z \\[2mm]
&= \; \int_{-z_b}^{z_b} \rho(l, 0) \exp\left(- GM\mu z^2/2\mathscr{R}Tl^3\right) \mathrm{d}z \\[2mm]
&= \; 0.843 \int_{-\infty}^{\infty} \rho(l, 0) \exp\left(- GM\mu z^2/2\mathscr{R}Tl^3\right) \mathrm{d}z \\[2mm]
&= \; 0.843\rho(l, 0)(2\pi\mathscr{R}Tl^3/GM\mu)^{1/2} \\[2mm]
&= \; 0.843\sigma,
\end{aligned} \tag{4.31}$$

where

$$\begin{aligned}
\sigma \; &= \; \int_{-\infty}^{\infty} \rho(l, z) \, \mathrm{d}z \\[2mm]
&= \; \rho(l, 0) \int_{-\infty}^{\infty} \exp\left(- GM\mu z^2/2\mathscr{R}Tl^3\right) \mathrm{d}z \\[2mm]
&= \; \rho(l, z)(2\pi\mathscr{R}Tl^3/GM\mu)^{1/2} \\[2mm]
&= \; \pi^{1/2}\rho(l, 0)z_b,
\end{aligned} \tag{4.32}$$

From Table II follows that the condition $z_b \lesssim l/3$ is fulfilled for the planetary system. Near the surface of the Sun Equation (4.30) becomes

$$z_{b\odot} \; = \; (2\mathscr{R}T_\odot R_\odot^3/GM\mu)^{1/2}, \; z_{b\odot}/R_\odot = 0.0145,$$

where $R_\odot$ is the radius, and $T_\odot$ the surface temperature, of the Sun.

If $z \gtrsim l/3$ we have from Equations (4.13) and (4.22)

$$\begin{aligned}
\rho(l, z) \; = \; &\rho(l_0, 0)(R^b l^{-3-b/2}/l_0^{-3+b/2}) \times \\
&\times \exp\left(GM\mu(l^{b-1} - R^{b-1})/\mathscr{R}A(b-1)\right), \; (z \gtrsim l/3).
\end{aligned}$$

If $b = \frac{1}{2}$ and A given by Equation (4.25) this equation yields values of the density which are well below those of interstellar clouds if $R < R_{\text{Pluto}}$, so that our approximation for $z \lesssim l/3$ from Equations (4.26)–(4.28) represents practically the whole protoplanetary cloud.

Table II shows that $\rho(l, 0)$ decreases by about six orders of magnitude if we move from

TABLE II

Characteristic values for the protoplanetary cloud, ($m_\oplus$ = Earth mass).

| l [AU]	Δl [AU]	m_{obs} [$m_\oplus$]	m_{in} [$m_\oplus$]	$\rho_{in}(l, 0)$ [g cm^{-3}]	$\rho(l, 0)$ [g cm^{-3}]	$\rho_{pb}(l, 0)$ [g cm^{-3}]	$\bar{\rho}$ [g cm^{-3}]	$\bar{\rho}_{pb}$ [g cm^{-3}]	σ [g cm^{-2}]	σ_p [g cm^{-2}]	z_b [AU]	z_b/l
0.39	0.34	0.055	31.0	2.65×10^{-9}	1.40×10^{-8}	4.81×10^{-11}	1.04×10^{-11}	3.58×10^{-11}	5290	18.1	0.014	0.037
0.72	0.30	0.815	259.3	6.20×10^{-9}	2.52×10^{-9}	8.65×10^{-12}	1.88×10^{-12}	6.44×10^{-12}	2070	7.10	0.030	0.043
1.00	0.40	1.000	300.0	2.60×10^{-9}	1.03×10^{-9}	3.52×10^{-12}	7.64×10^{-12}	2.62×10^{-12}	1270	4.36	0.047	0.047
1.52	0.74	0.108	32.1	5.76×10^{-11}	3.25×10^{-10}	1.11×10^{-12}	2.42×10^{-10}	8.28×10^{-13}	678	2.32	0.079	0.052
2.80	1.30	5×10^{-4}	0.1	3.66×10^{-14}	6.10×10^{-11}	2.09×10^{-13}	4.54×10^{-11}	1.56×10^{-13}	272	0.93	0.168	0.060
5.20	4.1	318.0	600	1.23×10^{-11}	1.11×10^{-11}	1.75×10^{-13}	8.27×10^{-12}	1.30×10^{-13}	107	1.70	0.364	0.070
9.54	7.0	95.1	1000	3.06×10^{-12}	2.07×10^{-12}	3.27×10^{-14}	1.54×10^{-12}	2.43×10^{-14}	43.9	0.68	0.780	0.082
19.19	10.3	14.6	700	3.29×10^{-13}	3.06×10^{-13}	4.83×10^{-15}	2.28×10^{-13}	3.60×10^{-15}	15.2	0.24	1.866	0.097
30.07	10.8	17.2	800	1.20×10^{-13}	8.86×10^{-14}	1.39×10^{-15}	6.59×10^{-14}	1.04×10^{-15}	7.7	0.12	3.273	0.109
39.50	8.0	0.1?	6.3	6.97×10^{-16}	4.25×10^{-14}	6.70×10^{-16}	3.16×10^{-14}	4.99×10^{-16}	5.2	0.08	4.580	0.117
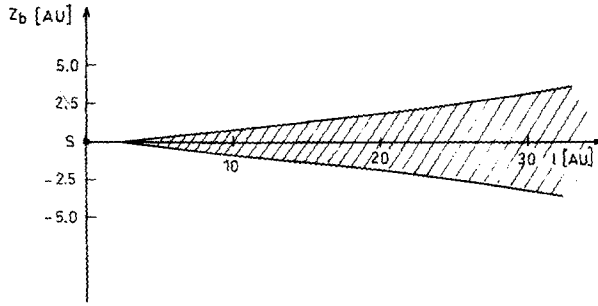
Fig. 1   Vertical cross-section of the protoplanetary cloud, (S denotes the Sun).

Mercury to Pluto. But because of the logarithmic dependence of z on $\rho(l, z)/\rho(l, 0)$, it is obvious that the variation of $\rho(l, 0)$ with l does not affect the order of magnitude of z_b. If the constant $1/e = 0.368$ from Equation (4.29) would be decreased maximally by six orders of magnitude to $1/10^{-6}e$, then z_b from Equation (4.30) increases only by the factor 3.7. So we could assume with good approximation that above height z_b the density drops rapidly below the values found in interstellar clouds and the mass of the cloud is concentrated with sufficient approximation in the disk shown in Fig. 1.

5. Opacity of the Protoplanetary Cloud

(i) *Early Stage.* An approximately reliable determination of the opacity of the proto-planetary cloud has been made only for the earliest stages, when small planetesimals similar to interstellar grains are present in cosmic abundance. For this case we assume a mean Rosseland opacity of $k = 0.15\,\text{cm}^2\text{g}^{-1}$ in the cloud (Larson, 1972b). However, even for this stage there are possible large variations of the opacity (Cameron and Pine, 1973, Figs. 5, 6).

In the early stage, the planetesimals are of interstellar grain size and well mixed with the gas. In this stage, the gas temperature is of the same order as the temperature of the planetesimals, provided that $\rho \gtrsim 10^{-22}\,\text{g cm}^{-3}$, (Larson, 1972b). This density delimitation is fulfilled practically for the whole protoplanetary cloud.

We discuss at first the opacity in the radial direction, when $R \simeq l$, i.e. $z \lesssim l/3$. The cloud is considered opaque to solar radiation if its optical depth τ between the distances l_1 and l_2 is larger than 2/3,

$$\tau = \int_{l_1}^{l_2} \kappa\rho(l, 0)\,\mathrm{d}l > 2/3. \tag{5.1}$$

With Equation (4.27) and $\kappa \approx \text{const}$, we obtain $(l_2\rho(l_2, 0) \ll l_1\rho(l_1, 0)$ from Table II)

$$\tau = 4\kappa l_1\rho(l_1, 0)/7 > 2/3 \quad \text{or} \quad \kappa l_1\rho(l_1, 0) > 7/6 \approx 1. \tag{5.2}$$

If we insert into Equation (5.2) the relevant density $\rho(l_1, 0)$ from Table II, we find that the optical depth is of order unity and below for the three outer planets ($10^{14}\,\text{cm} < l_1 < 6 \times 10^{14}\,\text{cm}$), while up to the region of Jupiter the optical depth is $\tau \gg 1$. The densities $\rho(l, 0)$ from Table II are lower limits so that the cloud could be completely opaque provided that $\kappa = 0.15\,\text{cm}^2\,\text{g}^{-1}$ if $z \lesssim z_b$.

If the protoplanetary cloud is transparent to solar radiation and when the small dust grains are well mixed with the gas, the temperature of gas and dust is given for the early stages with good approximation by Equation (3.8), (Larson, 1972b; Miki and Nakano, 1975).

If the protoplanetary cloud is opaque at the early stage it appears as a concave disk (see Fig. 1), whose surface is heated by solar radiation and starlight. The temperature T_b at the surface of the disk at level $z = z_b$ has been calculated by Kusaka et al. (1970)

$$T_b^4 = 2LR_\odot/3\pi^2 a_s cl^3 + (L/7\pi a_s c)^{8/7}(2\mathscr{R}/GM\mu l^3)^{4/7} + (4/l)\mathrm{d}((lz/3\kappa\rho)\,\mathrm{d}T^4/\mathrm{d}l)/\mathrm{d}l + T_{\text{ext}}^4,$$

$$(z \lesssim l/3). \tag{5.3}$$

The symbol $T_{\text{ext}} = 15\,\text{K}$ denotes the black-body temperature of an external radiation field, for instance from stars formed in the vicinity of the protoplanetary cloud. This external radiation field is appreciable only for the three outer planets, (Table I). Since there exists no published derivation of Equation (5.3) we note that the first term of this equation arises from heating by the Sun when $z_b \ll R_\odot$ and the second term when $z_b \gtrsim R_\odot$. Both terms can be determined in a straightforward manner from Safronov's (1969) textbook. The third term corresponds to the radiative energy flow inside the disk and was found to be negligible (Kusaka et al., (1970). It can be deduced by writing the radial radiation flow inside the protoplanetary cloud at distance l as $F = -(2\pi l z_b a_s c/3\kappa\rho)$ $\times \mathrm{d}T^4/\mathrm{d}l$ ($\tau \gg 1$, $z_b \lesssim l/3$), Kusaka personal communication). The main contribution to the temperature comes from the second term of Equation (5.3)

$$T_b \simeq (L/7\pi a_s c)^{2/7}(2\mathscr{R}/GM\mu)^{1/7}l^{-3/7} = \text{const} \times l^{-3/7}, \quad (z \lesssim l/3). \tag{5.4}$$

When the optical depth of the protoplanetary cloud is large in the equatorial plane at distance l it will be large also along the vertical z-direction in the vicinity of the equatorial plane up to the height z_b. In this case, the protoplanetary cloud can be approximated by a plane-parallel medium of large optical depth and the temperature T_b at height z_b is related to the temperature T_{be} in the equatorial plane by (Safronov, 1969, Chap. 4)

$$T_{be} = 3^{1/8}T_b/2^{1/2} = 0.81T_b, \quad (\tau \gg 1), \tag{5.5}$$

T_b and T_{be} both are prohibitively small if $L = L_\odot$ (see Table I) and would require a solar luminosity of several hundred $L_\odot$ to be in accordance with T_{chem} for the terrestrial planets. This could be an indication that the protoplanetary cloud was transparent for most time.

(ii) *Later Stage.* The small planetesimals grow to objects with radii 10^3–$10^4\,\text{cm}$ during 10^2–$10^5\,\text{yr}$, and settle towards the equatorial plane firming a disk of minimum

thickness 1–100 km, (see Sections 8–10). It is likely that the opacity of the protoplanetary cloud drops considerably when the radius of the planetesimals becomes large in comparison to the wavelength of radiation from the Sun, (Cameron and Pine, 1973). No calculations exist concerning this case which lasts for the overwhelming part of the accretion process (Tables III–IV). According to Equation (5.2) if $\kappa \lesssim 2 \times 10^{-5} \, \mathrm{cm^2 \, g^{-1}}$ the protoplanetary cloud is transparent outside Mercury's orbit, $(\rho(l_1, 0) \lesssim 10^{-8} \, \mathrm{g \, cm^{-3}}; \, l_1 > 6 \times 10^{12} \, \mathrm{cm}$; Table II). In this case, the condensation of gases onto the planetesimals is likely to be controlled by the black-body temperature from Equation (3.8), though the kinetic temperature of the gas at large distances from the planetesimals could be higher by orders of magnitude (e.g., Arrhenius and Alfvén, 1971). As it is obvious from Equation (4.30) the vertical boundary of the cloud z_b increases only as $T^{1/2}$, so that even for gas temperatures of several thousands degrees z_b increases only by the factor 3–4 with respect to the values from Table II. For our calculations, we have assumed that the temperature is given by Equation (3.8) for $L = L_\odot$, which should be regarded as a lower limit for the temperature of gas and dust during the accretion process. It will be obvious from the context of the paper that our results do not depend crucially on the temperature of gas and dust in the protoplanetary cloud.

Summarizing, during the earliest stages, the protoplanetary cloud could be opaque to solar radiation. But the planetesimals clump rapidly into larger ones and settle towards the equatorial plane, so that the cloud inside 50 AU is likely to be transparent during the accretion process of the planets. The temperature of the planetesimals is given by Equation (3.8) with a variable solar luminosity (Section 3), while the temperatures of the gas at large distances from the planetesimals could be considerably larger.

6. Initial Density Distribution in the Equatorial Plane

From Equations (4.16) and (4.28), we obtain for the mass of the protoplanetary cloud in a ring of width Δl

$$m = 4\pi l \Delta l \int_0^{z_b} \rho \, dz$$

$$\simeq 4\pi l \Delta l \int_0^\infty \rho \, dz$$

$$\simeq 4\pi l \rho(l, 0) \Delta l \int_0^\infty \exp\left(-GM\mu z^2 / 2\mathscr{R} A l^{5/2}\right) dz$$

$$= (8\pi^3 \mathscr{R} A / GM\mu)^{1/2} \rho(l, 0) l^{9/4} \Delta l, \quad (z_b \lesssim l/3). \tag{6.1}$$

We assume that approximately the whole accretable matter of the protoplanetary cloud passed into the actual planets, which accreted from adjacent concentric rings with the planet in the middle of each ring. m_{obs} in Table II denotes the actual observed

mass of the planet. From Weidenschilling's (1977b) Tables 1 and 2, we can deduce with m_{obs} the initial empirical mass m_{in} of gas, ice and dust corresponding to each planet. If we equate m_{in} from our Table II to m in Equation (6.1) we obtain with Δl from Table II the empirical initial density $\rho_{in}(l, 0)$ in the equatorial plane. Our values for the terrestrial planets are somewhat different from those of Weidenschilling (1977b) since we have assumed a mass fraction of Fe equal to 0.0011 (Podolak and Cameron, 1974; Table I).

For the determination of the surface density of planetesimals σ_p from Table II we make the fundamental assumption that inside the asteroid belt the planetesimals are formed only from the rocky fraction of the protoplanetary cloud (mass fraction 0.00343) and outside the asteroid belt from rock and ice (mass fraction 0.0158; Podolak and Cameron 1974; see also our Section 16).

For Pluto, we have $m_{in} = m_{obs}/0.0158$. We attribute little importance to all values concerning Pluto because of its uncertain origin (Horedt, 1974c) and of its small mass, which has suffered recent downward revision; it seems to be now of order $0.01m_\oplus$ rather than $0.1m_\oplus$ as we have assumed ($m_\oplus$ denoting the mass of the Earth).

The total mass of the protoplanetary cloud m_t is obtained from

$$m_t = 2\pi \int_{l_0}^{l} \int_{-z_b}^{z_b} l\rho(l, z) \, dl \, dz$$

$$\simeq 2\pi\rho(l_0, 0)l_0^{11/4} \int_{l_0}^{l} \int_{-\infty}^{\infty} l^{-7/4} \exp\left(-GM\mu z^2/2A\mathscr{R}l^{5/2}\right) dl \, dz$$

$$= (32\pi^3 \mathscr{R}A/GM\mu)^{1/2} \rho(l_0, 0)l_0^{11/4}l^{1/2}, \quad (l \gg l_0, z_b \lesssim l/3). \quad (6.2)$$

The empirical minimum total initial mass $m_{in,t}$ is obtained by adding together the empirical values m_{in} from Table II: i.e.,

$$m_{in,t} = 2.23 \times 10^{31} \text{g} = 0.011M. \quad (6.3)$$

Equating the empirical value $m_{in,t}$ to the theoretical value m_t from Equation (6.2), we obtain for $l_0 = 0.4$ AU equal to Mercury's distance from the Sun

$$\rho(l_0, 0) = 1.4 \times 10^{-8} \text{g cm}^{-3}, \quad l_0 = 5.8 \times 10^{12} \text{cm}; \quad (6.4)$$

and from Equation (4.27),

$$\rho(l, 0) = 1.40 \times 10^{-8}(l/5.80 \times 10^{12})^{-11/4}. \quad (6.5)$$

As seen from Figure 2, the theoretical density distribution from Equation (6.5) is smaller for the larger planets than the empirical density $\rho_{in}(l, 0)$ because of our averaging procedure. The low empirical density in the region of Mars and of the asteroids appears to be a secondary effect of the evolution of Jupiter (Safronov, 1969, Chap. 13; Horedt, 1974b; Weidenschilling, 1975). The low empirical density in the region of Mercury is probably a secondary effect due to the high temperature in this region, so that only solids with high melting point are accreted, (Weidenschilling, 1977b). Inside Mercury no planet could accrete because of the high temperature.
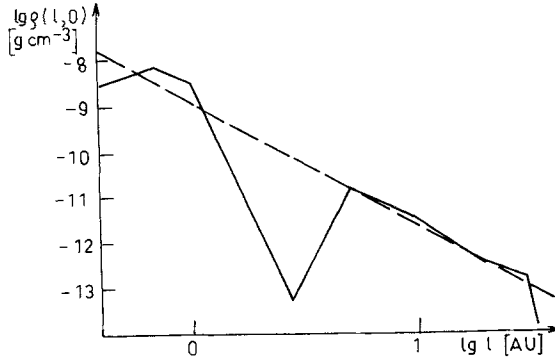
Fig. 2. Observational (continuous line) and theoretical (broken line) density distribution in the equatorial plane of the protoplanetary cloud.

The angular momentum K_t of the whole protoplanetary cloud is

$$K_t = \int_{l_0}^{l} \int_{-z_b}^{z_b} 2\pi\rho(l, z)l^3\omega \, dl \, dz$$

$$\simeq 2\pi(GM)^{1/2} \int_{l_0}^{l} \int_{-\infty}^{\infty} \rho(l, 0)l^{3/2} \exp\left(-GM\mu z^2/2\mathscr{R}Al^{5/2}\right) dl \, dz$$

$$= (8\pi^3 \mathscr{R} A/\mu)^{1/2}\rho(l_0, 0)l_0^{11/4}l$$

$$= m_t(GMl)^{1/2}/2, \quad (l \gg l_0, \quad z_b \lesssim l/3). \tag{6.6}$$

The angular velocity $\omega \approx (GM/l^3)^{1/2}$ is approximately equal to the circular Keplerian angular velocity. With m_t from Equation (6.2) we obtain the minimum angular momentum of the protoplanetary cloud

$$K_t = 3.07 \times 10^{51} \, \mathrm{g \, cm^2 \, s^{-1}}. \tag{6.7}$$

Pressure and density in the equatorial plane are connected by

$$p(l, 0) = p(l_0, 0)(\rho(l, 0)/\rho(l_0, 0))^{13/11},$$

as follows from Equations (3.3), (3.8) and (4.27).

7. Rotation of the Planets

To put into evidence the importance of the density distribution in the protoplanetary cloud for considerations regarding the axial rotation of the planets we write Equation (4.27) under the form

$$\rho(l, 0) = \rho(l_0, 0)(l/l_0)^c, \tag{7.1}$$

where $c = $ const. We assume as throughout this paper that the planet formed in the middle l of a ring between the distances $l(1 - e)$ and $l(1 + e)$, where e is the maximum eccentricity of planetesimals reaching the growing planet of mass M and radius r.

Analogous to Equation (6.6), we have for the angular momentum of the protoplanetary cloud between $l(1 - e)$ and $l(1 - e)$

$$K = (8\pi^3 \mathscr{R} A/\mu)^{1/2} \rho(l_0, 0) l^{(15/4)+c} ((1 + e)^{(15/4)+c} - (1 - e)^{(15/4)+c})/$$

$$((15/4) + c) l_0^c, \qquad (c \neq -15/4). \tag{7.2}$$

For the mass of the planet which we set equal to the mass of the protoplanetary cloud between $l(1 - e)$ and $l(1 + e)$ we have, by analogy with Equations (6.1) and (6.2),

$$m = (8\pi^3 \mathscr{R} A/GM\mu)^{1/2} \rho(l_0, 0) l^{(13/4)+c} ((1 + e)^{(13/4)+c}$$

$$- (1 - e)^{(13/4)+c})/((13/4) + c)) l_0^c, \quad (c \neq -13/4). \tag{7.3}$$

We assume the planetary spin axis to be directed along the z-axis and project the angular momentum on the z-axis; the orbital angular momentum of the protoplanetary cloud must be larger (because of dissipation) than the orbital angular momentum of the planet $m(GMl)^{1/2}$ plus its spin angular momentum $kmr^2 \omega_s$, where k $(k < 0.4)$ is the normalized radius of gyration and ω_s the spin angular velocity. Thus we have

$$K > m(GMl)^{1/2} + kmr^2 \omega_s. \tag{7.4}$$

We insert Equations (7.2) and (7.3) into Equation (7.4) and obtain after expansion up to e^3 ($e < 0.3$; Section 16)

$$P_s > 6kr^2 P/e^2 l^2 (2 + c), \quad (c \neq -2), \tag{7.5}$$

where $P_s = 2\pi/\omega_s$ and $P = 2\pi (l^3/GM)^{1/2}$ is the period of axial rotation and the orbital period, respectively.

We have excluded for our deduction the values $c = -15/4$ and $-13/4$. In these cases, we obtain a logarithmic relation for K and m, respectively, but the final result from Equation (7.5) is the same. If $c = -2$, we obtain by expanding Equations (7.2) and (7.3) up to the fifth power in e,

$$P_s > 1280 kr^2 P/e^4 l^2, \quad (c = -2). \tag{7.6}$$

If $c \simeq -2$ we have values between those from Equations (7.5) and (7.6). Equation (7.5) shows that if $c < -2$ there can occur also retrograde spins. As shown by Equation (7.6) the singularity for $c = -2$ occurs because of our analytical approximations. For our model of the cloud we have $c = -11/4$ and

$$P_s > -8kr^2 P/e^2 l^2. \tag{7.7}$$

From our equations it appears that the spin angular momentum of the planets is a small quantity of third order with respect to the eccentricity e ($e \ll 1$) of the planetismals. Our deduction shows also the crucial role of the density distribution in the protoplanetary cloud: for our density model there are possible, also retrograde spins.

I conclude that simple energy conservation laws are completely inadequate to determine a precise, reliable value of planetary spin, (e.g., Mitra, 1970; Horedt, 1975a). It appears that the problem of planetary spin can be investigated only along the lines developed by Giuli's (1968) numerical work (e.g., Kiladze, 1970; Harris, 1977).

8. Vertical Motion of Small Planetesimals ($r_b < r < r_1$)

When the radius of planetesimals is smaller than r_1 from Equation (9.6) the resistance of the gas is very large and the planetesimal is forced to rotate approximately together with the gas. Since $z \leqslant z_b \lesssim l/3$ for most planetesimals, it is possible to study the motion separately in the vertical z-direction and in the horizontal l-direction. This has been done in the present section and in the next one.

It is not quite clear whether interstellar grains could grow during collapse of an interstellar cloud (Horedt, 1975c; Scalo, 1977). In the region of the terrestrial planets most grains are likely to be vaporized, but as has been shown by Hartmann (1970), when the gas is cooling there condense rapidly planetesimals of interstellar grain size. When all condensable gases have been accreted onto small planetesimals, their further growth is a complicated task and could occur mainly by electrostatic and electromagnetic interaction (Arrhenius and Asunmaa, 1973; Coradini *et al.*, 1977) and by collisions. We make the most simple assumption that the planetesimals grow only by mutual collisions with collision efficiency 1, i.e. each impact is completely inelastic.

We start with a radius of the small planetesimal similar to the grain radii in interstellar clouds, namely $r_b = 10^{-5}$ cm in the region of the terrestrial planets and $r_b = 10^{-4}$ cm outside the asteroid belt. The planetesimals are assumed to be initially well mixed with the gas. Their mass fraction is taken equal $\lambda = 0.00343$ (fraction of rocky material) for the region of the terrestrial planets and $\lambda = 0.0158$ (fraction of rock and ice) for the outer planets, (Podolak and Cameron, 1974).

It appears convenient to define the mean density of the gas $\bar{\rho}(l)$ between the height $-z_b$ and z_b from Figure 1. This gas density is approximately equal to the total initial density of gas and dust, since dust constitutes at most 0.0158 fractions of the total mass. We average the gas density only between $-z_b$ and z_b because most planetismals move only between these heights, excepting perhaps for the later stages when $r > 10^3$ km and when the gas drag is relatively unimportant. In fact, the mean density $\bar{\rho}(l)$ between $-z_b$ and z_b is of the same order as the density in the equatorial plane, as follows from Equation (8.1): i.e.,

$$\bar{\rho} = \bar{\rho}(l) = \int_{-z_b}^{z_b} \rho(l, z) \, dz/2z_b$$

$$= 0.843 \int_{-\infty}^{\infty} \rho(l, 0) \exp\left(-GM\mu z^2/2\mathscr{R}Tl^3\right) dz/2z_b$$

$$= 0.421\pi^{1/2}\rho(l, 0) = 0.745\rho(l, 0). \tag{8.1}$$

The initial density of planetesimals in the equatorial plane is given by

$$\rho_{pb}(l, 0) = \lambda\rho(l, 0), \quad (\lambda = 0.00343 \text{ or } 0.0158). \tag{8.2}$$

The mean initial density of planetesimals between height $-z_b$ and z_b is from Equations (8.1) and (8.2)

$$\bar{\rho}_{pb}(l) = \lambda\bar{\rho}(l) = 0.421\pi^{1/2}\lambda\rho(l, 0) = 0.421\pi^{1/2}\rho_{pb}(l, 0). \tag{8.3}$$

For the early stages of accretion we consider only the planetesimals present initially between $-z_b$ and z_b. But the planetesimals settle towards the equatorial plane and for the later stages of accretion we can assume with good approximation that also planetesimals which were initially outside the heights $-z_b$ and z_b participate in the accretion process. Therefore, for the early stages (Sections 8–10), we consider only the truncated surface density σ_{pb} between height $-z_b$ and z_b. Its mathematical expression follows from Equations (4.31) and (8.2)

$$\sigma_{pb} = \lambda\sigma_b.. \tag{8.4}$$

The total surface density of planetesimals σ_p is related to the truncated surface density σ_{pb} by Equation (4.31)

$$\sigma_{pb} = 0.843\sigma_p, \tag{8.5}$$

where

$$\sigma_p = \int_{-\infty}^{\infty} \lambda\rho(l, z)\,\mathrm{d}z = \lambda\rho(l, 0)(2\pi\mathscr{R}Tl^3/Gm\mu)^{1/2} = \pi^{1/2}\rho_{pb}(l, 0)z_b \tag{8.6}$$

and

$$\sigma_{pb} = 0.843\pi^{1/2}\rho_{pb}(l, 0)z_b = 2\bar{\rho}_{pb}(l)z_b. \tag{8.7}$$

In view of the uncertainties of the problem, the distinction made in this paper between σ_{pb} and for the early stages and σ_p for the later stages seems to be superfluous. However, we are able to define only by this distinction a reasonable mean value for the density of planetesimals $\bar{\rho}_p$ which is representative for 85% of their mass.

The planetesimals settle towards the equatorial plane of the cloud and a grain initially at height z_b will reach after a certain interval the height z ($0 < z < z_b$). The conservation of mass is given by the constancy of the surface density $\sigma_{pb} = \text{const.}$, or from Equation (8.7)

$$\bar{\rho}_{pb}z_b = \bar{\rho}_p z, \tag{8.8}$$

where $\bar{\rho}_p$ is the mean density of planetesimals between the heights $-z$ and z. For the sake of simplicity we shall set $\bar{\rho}_p = \bar{\rho}_p(l)$.

Throughout this paper we take into account the resistance of the gas on the planetesimals, which appears to be important. The velocity with respect to the gas v of a spherical planetesimal of mass m and radius r changes due to the resistance P_i from the gas as

$$m \, dv/dt = -P_i, \quad (i = 1, 2, 3).\tag{8.9}$$

Due to their remarkable simplicity we have adopted for the resistance P_i the equations given by Williams and Crampin (1971), (see also Horedt, 1971, 1973c; Adachi *et al.*, 1976)

$$(4\pi\delta r^3/3) \, dv/dt = - \begin{cases} 4\pi\bar{\rho}Wr^2v/3 = P_1 & r \leqslant 3L_g/2 \ \ v \leqslant 4W/3, \\ 2\pi\bar{\rho}WL_grv = P_2 & \text{if} \ \ r \geqslant 3L_g/2, \ \ v \leqslant 2L_gW/r, \\ \pi\bar{\rho}r^2v^2 = P_3 & v \geqslant \text{Min}(4W/3, 2L_gW/r). \end{cases}\tag{8.10}$$

We are working only with spherical planetesimals of radius r and mass $m = 4\pi\delta r^3/3$, where δ denotes the uniform density: $\delta = 3 \, \text{g cm}^{-3}$ for the rock in the terrestrial region and $\delta = 1.5 \, \text{g cm}^{-3}$ for the rock and ice mixture in the region of the outer planets. $W = (8\mathscr{R}T/\pi\mu)^{1/2}$ is the mean thermal velocity of the gas, and $L_g = \mu m_H/2^{1/2}4\bar{\rho}\sigma_m$ the mean free length of path in the gas, where $m_H = 1.67 \times 10^{-24} \, \text{g}$ is the mass of the hydrogen atom and $\sigma_m = 10^{-15} \, \text{cm}^2$ is an approximate cross-section of the atoms and molecules of the gas. The viscosity of the gas is given by $\nu = \bar{\rho}WL_g/3$ (Williams and Crampin, 1971; Horedt, 1975c).

The value P_1 maximizes P_2 and P_3 as long as $v \leqslant 4W/3$. Therefore P_1 maximizes also the time of sedimentation towards the equatorial plane and we use P_1 for the resistance in this and in the following sections 9 and 10. The vertical motion of grains has already been studied (e.g., Safronov, 1969; Kusaka *et al.*, 1970) and we treat only briefly the three principal cases.

(i) Sedimentation without accretion of planetesimals ($r_b = r = $ const.). This case is only of theoretical interest, because the planets cannot form when no growth of planetesimals occurs. The equation of vertical motion under the influence of the gas drag P_1 and the solar gravitation $GM/R^2 \simeq GM/l^2$, ($z \leqslant z_b \gtrsim l/3$) is

$$d^2z/dt^2 + (\bar{\rho}W/\delta r_b) \, dz/dt + GMz/l^3 = 0.\tag{8.11}$$

With the initial conditions $z = z_b$, $dz/dt = 0$, if $t = 0$, we obtain

$$z = z_b \exp\left(-GMr_b\delta t/l^3\bar{\rho}W\right) - (z_bGM\delta^2r_b^2/l^3\bar{\rho}^2W^2) \times$$

$$\times \exp\left(-\bar{\rho}Wt/r_b\delta\right) \simeq z_b \exp\left(-GM\delta r_b t/l^3\bar{\rho}W\right);\tag{8.12}$$

because for our numerical values $GMr_b^2\delta^2 \ll \bar{\rho}^2W^2l^3$. The density changes with Equation (8.8) as

$$\bar{\rho}_p = \bar{\rho}_{pb} \exp\left(GM\delta r_b \, t/l^3\bar{\rho}W\right).\tag{8.13}$$

(ii) Growth proportional to the thermal velocity of planetesimals, ($dr/dt \propto W_p$). This assumption has been used by Kusaka *et al.* (1970) though it appears that $|dz/dt|$ is for our numerical examples considerably larger than the thermal velocity of planetesimals W_p, (see Case (iii)). We have

$$W_p = (9k_B T/4\pi r^3 \delta)^{1/2},$$ (8.14)

where $k_B = 1.38 \times 10^{-16}$ erg/degree denotes the Boltzmann constant. The accretion is given by (we take $\bar{\rho}_{pb}$ instead of $\bar{\rho}_p$, see Case (iii))

$$dr/dt = \bar{\rho}_{pb} W_p/4\delta = (3\bar{\rho}_{pb}/8)(k_B T/r^3 \pi \delta^3)^{1/2}.$$ (8.15)

The integral of Equation (8.15) is

$$r = (r_b^{5/2} + (15\bar{\rho}_{pb}/16)(k_B T/\pi\delta^3)^{1/2} t)^{2/5}.$$ (8.16)

As will be shown in the next case (iii) the term dz^2/dt^2 is negligible with respect to the other terms, so that Equation (8.27) can be used

$$dz/dt = -GMr\delta z/\bar{\rho} W l^3.$$ (8.17)

Introducing Equation (8.16) into Equation (8.17) and integrating, we get

$$t = (16/15\bar{\rho}_{pb})(\pi\delta^3/k_B T)^{1/2} \times$$

$$\times [((21\bar{\rho}_{pb}\bar{\rho} l^3 W/16GM\delta^{5/2})(k_B T/\pi)^{1/2} \ln (\bar{\rho}_p/\bar{\rho}_{pb}) + r_b^{7/2})^{5/7} - r_b^{5/2}].$$
                                   (8.18)

The time $t_b (dr/dt \propto W_p)$ necessary for the density $\bar{\rho}_{pb}$ to grow to $e\bar{\rho}_{pb}$ and the corresponding radius r from Equation (8.16) are listed in Table III. The most rapid grain growth is obtained by the most plausible assumption from the next case.

(iii) Growth of planetesimals proportional to sedimentation velocity $(dr/dt \propto dz/dt)$. The numerical integration offers somewhat different results for this case in comparison to analytical evaluations, but the general trend of the results is preserved (e.g., Williams and Crampin, 1971). We have assumed that the relative velocity between the planetesimals is equal to their sedimentation velocity with respect to the Sun $-dz/dt$. The accretion rate becomes

$$dm/dt = 4\pi\delta r^2 dr/dt = -\pi r^2 \bar{\rho}_p dz/dt.$$ (8.19)

With Equation (8.8), we can integrate Equation (8.19)

$$r - r_b = (z_b \bar{\rho}_{pb}/4\delta) \ln (z_b/z).$$ (8.20)

If we put in Equation (8.19) $\bar{\rho}_p = \bar{\rho}_{pb} = $ const., we obtain

$$r - r_b = \bar{\rho}_{pb}(z_b - z)/4\delta,$$ (8.21)

and the maximum radius if $z \ll z_b$ is

$$r_{max} = \bar{\rho}_{pb} z_b/4\delta.$$ (8.22)

Equation (8.20) cannot be used for further analytical evaluations because of the logarithmic term. We use Equation (8.21) instead of Equation (8.20); in fact because of the logarithmic dependence in Equation (8.20) the maximum radius given by Equation (8.20) is for any reasonable value of z_b/z only about ten times larger than r_{max} from Equation (8.22). The equation of motion is similar to Equation (8.11)

TABLE III

Characteristic heights, velocities, radii, densities and time intervals for the first stages of accretion. $(r_b \leqslant r \leqslant r_1)$.

I. Vertical motion

Planet	t_b [yr]	t_b [yr]	t_b [yr]	r_{max} [cm]	r [cm]
	$r = $ const.	$dr/dt \propto W_p$	$dr/dt \propto dz/dt$	$dr/dt \propto dz/dt$	$dr/dt \propto W_p$
Mercury	3.21×10^6	1.56×10^4	5.77×10^2	6.35×10^{-1}	2.88×10^{-3}
Venus	3.21×10^6	2.68×10^4	1.37×10^3	2.49×10^{-1}	1.70×10^{-3}
Earth	3.21×10^6	3.55×10^4	2.14×10^3	1.53×10^{-1}	1.28×10^{-3}
Mars	3.21×10^6	5.10×10^4	3.76×10^3	8.13×10^{-2}	8.93×10^{-4}
Asteroids	3.21×10^6	8.57×10^4	8.48×10^3	3.28×10^{-2}	5.31×10^{-4}
Jupiter	6.42×10^5	1.16×10^5	4.11×10^3	1.19×10^{-1}	7.98×10^{-4}
Saturn	6.42×10^5	1.94×10^5	9.02×10^3	4.75×10^{-2}	4.71×10^{-4}
Uranus	6.42×10^5	3.54×10^5	2.17×10^4	1.68×10^{-2}	2.67×10^{-4}
Neptune	6.42×10^5	5.19×10^5	3.75×10^4	8.52×10^{-3}	1.91×10^{-4}
Pluto	6.42×10^5	6.53×10^5	5.14×10^4	5.72×10^{-3}	1.15×10^{-4}

II. Horizontal motion

Planet	t_1 [yr]	r_1 [cm]	$\bar{r}$ [cm]	$\bar{\rho}_{p1}$ [g cm^{-3}]	z_1 [cm]	$|dl/dt|_1$ [cm s^{-1}]	$l_b - l_1$ [cm]
Mercury	8.34×10^2	61.1	4.21×10^{-5}	9.42×10^{-9}	8.08×10^8	5.11×10^2	9.25×10^6
Venus	2.00×10^3	66.3	4.77×10^{-5}	1.46×10^{-9}	2.05×10^9	1.41×10^3	6.37×10^7
Earth	3.14×10^3	81.3	5.11×10^{-5}	5.52×10^{-10}	3.31×10^9	2.82×10^3	1.75×10^8
Mars	5.60×10^3	105	5.63×10^{-5}	1.59×10^{-10}	6.16×10^9	6.86×10^3	6.46×10^8
Asteroids	1.30×10^4	155	6.69×10^{-5}	2.64×10^{-11}	1.49×10^{10}	2.50×10^4	4.41×10^9
Jupiter	6.43×10^3	214	6.47×10^{-4}	1.66×10^{-11}	4.30×10^{10}	4.37×10^4	2.68×10^{10}
Saturn	1.44×10^4	85.2	6.99×10^{-4}	2.49×10^{-12}	1.15×10^{10}	4.37×10^4	1.63×10^{11}
Uranus	3.64×10^4	30.1	7.66×10^{-4}	2.87×10^{-13}	3.51×10^{11}	4.37×10^4	1.27×10^{12}
Neptune	6.51×10^4	15.3	8.10×10^{-4}	6.99×10^{-14}	7.32×10^{11}	4.37×10^4	4.76×10^{12}
Pluto	9.12×10^4	10.2	8.46×10^{-4}	3.04×10^{-14}	1.13×10^{12}	4.37×10^4	1.04×10^{13}

$$d(m\, dz/dt)/dt + m\bar{\rho}W\, dz/r\delta\, dt + mGMz/l^3 = 0; \tag{8.23}$$

or, using Equation (8.19) with $\bar{\rho}_p = \bar{\rho}_{pb}$, $(\bar{\rho}_{pb} = \lambda\bar{\rho})$,

$$d^2z/dt^2 + (\bar{\rho}W/r\delta)(1 - (3\lambda/4W)\, dz/dt)\, dz/dt + GMz/l^3 = 0. \tag{8.24}$$

Because $|dz/dt| < 4W/3$ and $\lambda \ll 1$, we have $(3\lambda/4W)|dz/dt| \ll 1$. With a suitable mean value $\bar{r}$ of r Equation (8.24) becomes analogous to Equation (8.11): i.e.,

$$d^2z/dt^2 + (\bar{\rho}W/\bar{r}\delta)\, dz/dt + GMz/l^3 = 0; \tag{8.25}$$

with the solution, analogous to Equation (8.12), of the form

$$z \simeq z_b \exp(-GM\delta\bar{r}t/l^3\bar{\rho}W). \tag{8.26}$$

But this solution is identical to the solution of Equation (8.24) without the first term d^2z/dt^2 if $r = \bar{r}$. We conclude that the first term in Equation (8.24) is negligible so that Equation (8.24) can be written approximately as

$$(\bar{\rho}W/r\delta)\,dz/dt + GMz/l^3 = 0. \tag{8.27}$$

With Equation (8.19) the solution of Equation (8.27) is found to be

$$t = (\bar{\rho}Wl^3/GM\delta r_b\,(1 + \bar{\rho}_{pb}z_b/4\delta r_b))$$

$$\times \ln\left[z_b(1 + \bar{\rho}_{pb}(z_b - z)/4\delta r_b)/z\right],\ z < z_b \tag{8.28}$$

For our numerical examples we have $\bar{\rho}_{pb}z_b/4\delta r_b \gg 1$, so that even in the logarithmic term of Equation (8.28) $\bar{\rho}_{pb}(z_b - z)/4\delta r_b$ becomes the leading term if $z \not\approx z_b$, $(z < z_b)$. Therefore, by using Equation (8.8), Equation (8.28) becomes

$$t \simeq (4l^3W/\lambda GMz_b)\ln\,(z_b(\bar{\rho}_p - \bar{\rho}_{pb})/4\delta r_b),\quad (\bar{\rho}_p \not\approx \bar{\rho}_{pb},\ \bar{\rho}_p > \bar{\rho}_{pb})$$

and $$\tag{8.29}$$

$$\bar{\rho}_p \simeq \bar{\rho}_{pb} + (4\delta r_b/z_b)\exp\,(\lambda GMz_bt/4l^3W) = \bar{\rho}_{pb} + \beta\exp\alpha t, \tag{8.30}$$

where

$$\bar{\rho}_{pb} \not\approx \bar{\rho}_p.\qquad \alpha = \lambda GMz_b/4l^3W,\quad \beta = 4\delta r_b/z_b.$$

The time interval t_b needed to increase $\bar{\rho}_b$ by the factor e is listed in Table III. From Equations (8.8) and (8.30) we obtain a simple expression for the sedimentation velocity

$$dz/dt = \bar{\rho}_{pb}z_b\,d(1/\bar{\rho}_p)/dt = -\alpha z,\quad (z \not\approx z_b), \tag{8.31}$$

which is smaller than $4W/3$, so that P_1 is indeed a reliable approximation to the gas drag.

9. Horizontal Motion of Small Planetesimals $(r_b < r < r_1)$

For radii smaller than r_1 from Equation (9.6), the resistance of the gas is so large that the tangential motions with respect to the gas of the protoplanetary cloud are efficiently damped. Therefore, we can neglect the tangential motion of planetesimals with respect to the radial motion in a plane parallel to the equatorial plane. We introduce in this plane a rectangular (x, y)-frame, rotating together with the gas of the cloud at angular speed ω. The equations of motion projected on the coordinate axes are (e.g., Horedt, 1973a) with $z \lesssim l/3$

$$d(m\,dx/dt)dt + P_{ix} + (mGM/l^3 - m\omega^2)x - 2m\omega\,dy/dt = 0, \tag{9.1}$$

$$d(m\,dy/dt)/dt + P_{iy} + (mGM/l^3 - m\omega^2)y - 2m\omega\,dx/dt = 0, \tag{9.2}$$

where P_{ix} and P_{iy} are the projections of P_i $(i = 1, 2, 3)$ from Equation (8.10). Because of the reasons outlined above is sufficient to study the motion only radially, so that we can neglect one of the equations (9.1) and (9.2). If we take, for instance, the radial direction along the x-axis, we can neglect also the last term in Equation (9.1) and replace x by l: i.e.,

$$d(m \, dl/dt)/dt + P_1 + (mGM/l^3 - m\omega^2)l = 0, \tag{9.3}$$

where $P_i = P_{il}$ and we have taken as in the previous section $i = 1$. If we replace m in Equation (9.3) by a mean value $\bar{m}$, we can show exactly as for Equation (8.23) that the first term is negligible so that Equation (9.3) becomes by using Equation (4.23)

$$(4\pi\bar{\rho}Wr^2/3) \, dl/dt = -ml(GM/l^3 - \omega^2) = -13\pi\delta r^3 \mathscr{R}A/3\mu l^{3/2}$$

or

$$dl/dt = -13\delta r\mathscr{R}A/4\mu\bar{\rho}Wl^{3/2}. \tag{9.4}$$

Equation (9.4) characterizes approximately the horizontal inward motion of a planetesimal under the influence of gravitation and of large resistance from the gas which rotates circularly with speed V_g. The resistance P_1 maximizes P_2 and P_3 ($v < 4W/3$) so it decreases the velocity of inward motion and the time of accretion. In fact P_1 is valid for the whole planetary system if $r \approx r_b$ and up to $r \approx r_1$ for the outer planets.

We determine the approximate maximum radius r_1 up to which the planetesimal can be considered to rotate together with the gas, i.e. the approximate limit at which gas drag becomes small in comparison to the gravitation from the Sun. We define r_1 conveniently by the condition that the velocity v of the planetesimal with respect to the gas decreases e-times during a period of orbital revolution

$$P = 2\pi(l^3/GM)^{1/2}. \tag{9.5}$$

The motion of a planetesimal under the influence of gas drag alone is given in Equation (8.9). If we integrate Equation (8.9) for $r = r_1$ by using Equation (8.10) and the condition $v_0/v = e$, $(v|_{t=0} = v_0)$ we find (*cf.* Whipple, 1972)

$$r_1 = \begin{cases} \bar{\rho}WP/\delta & r_1 \leqslant 3L_g/2; \; v_0 \leqslant 4W/3 \\ (3\bar{\rho}WL_gP/2\delta)^{1/2} & \text{if} \quad r_1 \geqslant 3L_g/2; \; v_0 \leqslant 2L_gW/r_1, \\ 3P\bar{\rho}v_0/4(e-1) & v_0 \geqslant \text{Min} \, (4W/3; \; 2L_gW/r_1) \end{cases} \tag{9.6}$$

The characteristic relative velocity between planetesimals and gas is taken equal to $v_0 = V_c - V_g = 5.25 \times 10^3 \, \text{cm s}^{-1}$ from Equation (4.24). Though the definition of r_1 is somewhat arbitrary it can be considered as a reasonable delimitation between two distinct regimes of motion: if $r_b \leqslant r \leqslant r_1$ the motion of planetesimals is slow with respect to the circular velocity of the gas V_g, and if $r > r_1$ the motion is essentially a Keplerian ellipse perturbed by a relatively small resistance from the gas.

The radius of the planetesimals increases according to

$$dr/dt = -(\bar{\rho}_p/4\delta) \, dl/dt = 13\mathscr{R}Ar(\bar{\rho}_{pb} + \beta \exp \alpha t)/16\mu\bar{\rho}Wl^{3/2}. \tag{9.7}$$

The inward velocity $-dl/dt$ approximates only very grossly the relative velocity between planetesimals, analogous to $-dz/dt$ in the preceding section. It is obvious from Table III that accretion is much more efficient in the horizontal direction than in

the vertical direction. Therefore, we have integrated Equation (9.7) between r_b and r_1 instead between r_{max} from Equation (8.22) and r_1

$$\ln (r_1/r_b) \simeq 13\mathscr{R}A(\bar{\rho}_{pb}t_1 + \beta(\exp \alpha t_1 - 1)/\alpha)/16\mu\bar{\rho}Wl^{3/2}, \text{ if } \bar{\rho}_{p1} \not\approx \bar{\rho}_{pb},$$
(9.8)

and

$$\ln (r_1/r_b) \simeq 13\mathscr{R}A\bar{\rho}_{p1}/16\mu\bar{\rho}Wl^{3/2}\alpha \quad \text{if} \quad \bar{\rho}_{p1} \gg \bar{\rho}_{pb}.$$
(9.9)

Because $\bar{\rho}_{p1} \gg \bar{\rho}_{pb}$ we have calculated t_1 from Table III according to, (cf. Equation 8.30))

$$t_1 \simeq \ln (\bar{\rho}_{p1}/\beta)/\alpha.$$
(9.10)

The length of inward motion can be obtained by introducing into Equation (9.4) a suitable mean radius $\bar{r}$ of the planetesimals during the time interval t_1. The integral of Equation (9.7) between an arbitrary radius r and r_b is

$$r = r_b \exp [13\mathscr{R}A(\bar{\rho}_{pb}t + \beta(\exp \alpha t - 1)/\alpha)/16\mu\bar{\rho}Wl^{3/2}].$$
(9.11)

We can deduce the mean radius $\bar{r}$ by averaging the time dependent part of Equation (9.11) over the interval t_1: i.e.,

$$\bar{\rho}_{pb}t + \beta(\exp \alpha t - 1)/\alpha = \int_0^{t_1} (\bar{\rho}_{pb}t + \beta(\exp \alpha t - 1)/\alpha) \, dt/t_1.$$

Performing the integration and introducing the result to Equation (9.11) we find that

$$\bar{r} = r_b \exp (13\mathscr{R}A(\bar{\rho}_{pb}t_1/2 + \bar{\rho}_{p1}/\alpha^2 t_1 - \beta/\alpha)/16\mu\bar{\rho}Wl^{3/2}).$$
(9.12)

The distance of inward motion is (Table III)

$$l_b - l_1 = 13\delta\bar{r}\mathscr{R}At_1/4\mu\bar{\rho}Wl^{3/2},$$
(9.13)   (9.13)

where l_b denotes the value of l at the initial moment corresponding to r_b and, $l_1 = l(t_1)$. A more detailed expression for Equation (9.7) would be

$$dr/dt = -(\bar{\rho}_p/4\delta)(dl/dt)(1 + 8\pi\delta Gr^2/3(dl/dt)^2);$$
(9.13)

but the second term in the paranthesis, the gravitational accretion term, is completely negligible.

From the values listed in Table III we could draw the following conclusions: The planetesimals grow during 10^3-10^5 yr up to meter-sized objects, mainly because of their horizontal motion. The accretion due to the motion in the vertical direction is not so important but increases considerably the spatial density of planetesimals, which becomes comparable to the gas density in the vicinity of the equatorial plane after the interval t_1.

10. Further Contraction Towards the Equatorial Plane $(r_1 \leqslant r \leqslant r_2)$

We have introduced this section in order to bridge the gap between the stage when the planetesimals begin to move in Keplerian orbits and the stage when gravitational interactions

between the planetesimals become important. During this stage the radius increases 100–1000 times (Table IV) but it is questionable if our model is very realistic because the planetesimals are likely to differ grossly in size and in the inclination i of their orbits with respect to the equatorial plane of the cloud. The planetesimals are assumed to move in approximately circular Keplerian orbits of inclination

$$i \simeq \mathrm{tg}\, i = z/l, \qquad (z \lesssim l/3), \tag{10.1}$$

where z is the maximum height attained by the planetesimals ($z = \bar{\rho}_{pb} z_b / \bar{\rho}_p$).

I was not able to solve the problem whether the gas between height $-z$ and z maintains its velocity difference $V_c - V_g$ with respect to the approximately circular velocity of the planetesimals V_c. On the one hand, the density of planetesimals near the equatorial plane increases from the value $\bar{\rho}_{p1} \approx \bar{\rho}$ at moment t_1 to $\bar{\rho}_{p2} \approx 10^4 \bar{\rho}$ at moment t_2 (Table IV). The mass of planetesimals between $-z$ and z becomes considerably larger than the mass of the gas, so that the planetesimals could accelerate the gas up to their velocity V_c. On the other hand, the mean distance between the planetesimals is even at moment t_2 and at Mercury's distance from the Sun about 20 times larger than their dimensions, so that the gas could maintain its velocity V_g.

I made the assumption that because the planetesimals constitute at most 1.6% of the whole cloud mass, the gas of the cloud readjusts its velocity by internal cloud motion in order to maintain also near the equatorial plane the velocity difference $V_c - V_g$ required by hydrostatic equilibrium.

We could have made also the alternative assumption that the gas between height $-z$ and z is accelerated by planetesimals up to their velocity V_c, though in this case no equilibrium configuration is possible within the limit of our assumptions. In this case, the evolution of the disk of planetesimals would occur by mutual collisions, without gas drag. The evolution time is in this case several orders of magnitude larger because the relative velocity between planetesimals is U_i instead of $-\mathrm{d}l/\mathrm{d}t$, ($U_i \ll |\mathrm{d}l/\mathrm{d}t|$; see Equation (10.14)).

We reproduce below only the equations written under the assumption that the gas continues to move with velocity V_g also between height $-z$ and z. The resistance is given as before by P_1, though for the inner planets P_2 and P_3 are more appropriate. P_1 maximizes P_2 and P_3 since the relative velocity between gas and planetesimals is $v = V_c - V_g \ll 4W/3$, neglecting the influence of small orbital inclinations. Because gravitational perturbations are small, the planetesimals move in nearly circular orbits. The semimajor axis of a planetesimal can be approximated by l since $z \ll l$ and its decrease due to gas drag is given (cf. Equation (14.1) by

$$-\,\mathrm{d}l/\mathrm{d}t = 2P_1 (l^3/GM)^{1/2}/m = 2\bar{\rho} W (V_c - V_g)(l^3/GM)^{1/2}/r\delta. \tag{10.2}$$

The relative velocity between planetesimals is given as in the preceding section by $-\mathrm{d}l/\mathrm{d}t$, because the relative velocity introduced from the difference in inclination U_i is about 10^2–10^3 times smaller, as it is obvious from Equation (10.14). The decrease in inclination due to gas drag (cf. Equation (14.3)) is given by

TABLE IV

Heights, velocities, radii, densities and time intervals for the intermediary stage of accretion ($r_1 \leqslant r \leqslant r_2$)

Planet	$t_2 - t_1$ [yr]	r_2 [cm]	r_{grav} [cm]	$\bar{\rho}_{p_2}$ [g cm^{-3}]	z_2 [km]	$|dl/dt|_2$ [cm s^{-1}]	$l_1 - l_2$ [AU]
Mercury	8.70	9.42×10^4	1.74×10^4	4.44×10^{-5}	1.72	92.7	0.014
Venus	35.3	5.92×10^4	1.27×10^4	1.09×10^{-6}	2.73	58.2	0.038
Earth	73.9	4.63×10^4	1.08×10^4	5.22×10^{-6}	3.50	45.5	0.064
Mars	190	3.38×10^4	8.75×10^3	2.04×10^{-6}	4.81	33.3	0.125
Asteroids	744	2.14×10^4	6.48×10^3	5.19×10^{-7}	7.57	21.1	0.326
Jupiter	2.53×10^3	2.27×10^4	7.54×10^3	1.08×10^{-7}	66.0	15.8	0.770
Saturn	9.94×10^3	1.43×10^4	5.55×10^3	2.74×10^{-8}	104	10.0	1.95
Uranus	4.76×10^4	8.52×10^3	3.92×10^3	5.74×10^{-9}	175	5.9	4.80
Neptune	1.31×10^5	6.05×10^3	3.13×10^3	2.08×10^{-9}	245	4.2	9.20
Pluto	2.40×10^5	4.96×10^3	2.74×10^3	1.14×10^{-9}	301	3.4	13.5
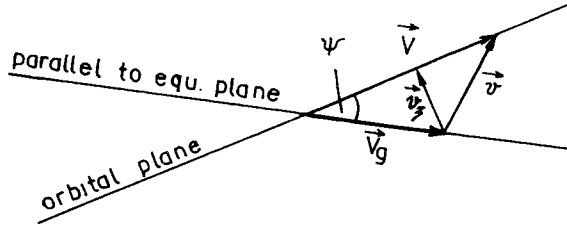
Fig. 3.   Velocity vectors for the intermediary stage of accretion $(r_1 \leqslant r \leqslant r_2)$

$$\mathrm{d}i/\mathrm{d}t = -(l/GM)^{1/2} \cos u P_{1\zeta}/m, \qquad (10.3)$$

where $P_{1\zeta}$ is the component of P_1 perpendicular to the orbital plane and u the angle between the planetesimal and the node of its orbit. We have neglected the contribution of colliding planetesimals to the decrease of $\mathrm{d}i/\mathrm{d}t$ because in this case the perturbing force is given by P_3 instead of P_1 and $P_3 \ll P_1$. We have

$$P_{1\zeta} = 4\pi\bar{\rho}Wr^2 v_\zeta/3m, \qquad (10.4)$$

where v_ζ is the component of v perpendicular to the orbital plane. From Figure 3 and the spherical triangle containing the orbit of the planetesimal and of the equator we get

$$v_\zeta = V_g \sin\psi = V_g \sin i \cos u/(1 - \sin^2 u \sin^2 i)^{1/2} \simeq V_c i \cos u, \quad (10.5)$$

because $i \approx 0$ and $(V_c - V_g)/V_c \ll 1$. From Equations (10.3), (10.4) and (10.5) we get

$$\mathrm{d}i/\mathrm{d}t = -\bar{\rho}Wi\cos^2 u/r\delta. \qquad (10.6)$$

Differentiating Equation (10.1) we get from Equation (8.8)

$$\mathrm{d}i/\mathrm{d}t = -(z_b\bar{\rho}_{pb}/l\bar{\rho}_p^2)(\mathrm{d}\bar{\rho}_p/\mathrm{d}t). \qquad (10.7)$$

Equating Equation (10.6) to (10.7) and using Equations (8.8) and (10.1), we obtain for the increase of density the expression

$$\mathrm{d}\bar{\rho}_p/\mathrm{d}t = \bar{\rho}_p\bar{\rho}W/2r\delta, \qquad (10.8)$$

where we have introduced instead of $\cos^2 u$ its mean value $1/2$. The radius of the planetesimal increases according to

$$\mathrm{d}r/\mathrm{d}t = -(\bar{\rho}_p/4\delta)\,\mathrm{d}l/\mathrm{d}t = \bar{\rho}\bar{\rho}_p W(V_c - V_g)(l^3/GM)^{1/2}/2r\delta^2. \qquad (10.9)$$

Dividing Equations (10.8) and (10.9) we obtain by integration

$$r_2 - r_1 = (l^3/GM)^{1/2}(V_c - V_g)(\bar{\rho}_{p2} - \bar{\rho}_{p1})/\delta, \qquad (10.10)$$

where r_2 and $\bar{\rho}_{p2}$ are the radius and the density at moment t_2. The radius r_2 is determined

only by Equation (13.15). Introducing Equation (10.10) into Equation (10.9) we have (Table IV)

$$t_2 - t_1 = (2\delta/\bar{\rho}W)$$

$$\times [r_2 - r_1 + (\bar{\rho}_{p1}(V_c - V_g)(l^3/GM)^{1/2}/\delta - r_1) \ln (\bar{\rho}_{p1}/\bar{\rho}_{p2})];$$

or, since $r_2 \gg r_1$ and $\bar{\rho}_{p2} \gg \bar{\rho}_{p1}$,

$$t_2 - t_1 = 2\delta r_2/\bar{\rho}W. \tag{10.11}$$

The variation $l_1 - l_2$ of the distance from the Sun is very large for Neptune and Pluto ($\approx l/3$; Table IV) but in view of the many uncertainties of this stage we do not attribute too much importance to this fact. From Equations (10.2) and (10.9) we find by integration

$$l_2^{-1/2} = l_1^{-1/2} + 2(V_c - V_g) \ln (\bar{\rho}_{p2}/\bar{\rho}_{p1})/(GM)^{1/2}. \tag{10.12}$$

The relative velocity which would appear from the difference in inclination is (Figure 3)

$$U_i = V_c|\sin \psi| = (GM/l)^{1/2}|i \cos u| = 2z_b\bar{\rho}_{pb}(GM/l^3)^{1/2}/\pi\bar{\rho}_p, \tag{10.13}$$

where we have used the mean value $2/\pi$ of $|\cos u|$ and also Equations (8.8) and (10.1). Comparing Equations (10.2) and (10.13) and using Equation (10.10) in the form

$$r \simeq (l^3/GM)^{1/2}(V_c - V_g)\bar{\rho}_p/\delta,$$

we find that the condition

$$|dl/dt| \gg U_i$$

is fulfilled always for our numerical examples: namely,

$$\pi\bar{\rho}W(l^3/GM)^{1/2}/z_b\bar{\rho}_{pb} \gg 1. \tag{10.14}$$

The radius at which gravitational accretion becomes important is from Equation (9.13)

$$8\pi\delta Gr^2/3(dl/dt)^2 \gtrsim 1,$$

or, with Equation (10.2),

$$r = r_{\text{grav}} \gtrsim (3\bar{\rho}Wl^{3/2}(V_c - V_g)/4\pi\delta^2 G^{3/2}M^{1/2})^{1/3}. \tag{10.15}$$

As is shown in Table IV this radius is $\gg r_1$ and comparable to r_2 so that the simple Equation (10.9) is valid approximately if $r \lesssim r_2$, giving a lower limit to the accretion rate. As it is obvious from Tables III and IV the planetesimals reach radii of 0.1–1 km during several hundred years for Mercury and several 10^5 yr for Pluto.

11. Velocity Dispersion by Close Encounters

Before turning to the late stages of planetary accretion ($r_2 \lesssim r \lesssim r_3$) we develop a crude theory in order to obtain the increase of the relative velocity U between planetesimals by gravitational encounters. Strictly speaking, by mutual encounters there occurs

merely a statistical increase of the dispersion of the velocities according to a quadratic sum rule, i.e. if we start with a small relative velocity U_{in} and assume that after each encounter the relative velocity U_k changes by ΔU_k, then after a large number n of encounters, the expectation of U^2 equals the quadratic sum of the individual deflections ΔU_k

$$U^2 = \sum_{k=1}^{n} (\Delta U_k)^2, \quad (|\Delta U_k| \ll U_k; U \gg U_{in}). \tag{11.1}$$

We consider only encounters occurring inside the gravitational sphere of action (Öpik, 1966a)

$$s_g = R(m/2M)^{1/3}, \tag{11.2}$$

or

$$s_g \simeq l(m/2M)^{1/3}, \qquad (z \lesssim l/3). \tag{11.3}$$

When a large planetesimal moves in a circular orbit and encounters within the framework of the circular restricted three body problem a small planetesimal their relative velocity before and after encounter is invariant, (e.g., Horedt, 1972a, b; 1974a). This idealized case occurs only approximately in the actual planetary system and was certainly absent during accretion of the planets, because of the large number of encountering planetesimals. Changes of the relative velocity U by encounters can occur only within the framework of the eccentric three or many body problem.

Let us consider a rotating (R, φ, ζ)-frame with the centre in the planetesimal. Let the R-axis be directed along the vector Sun-planet, the φ-axis in the orbital plane at right angle to the R-axis and the ζ-axis perpendicular to the orbital plane of the planetesimal.

At distance R the semimajor axis a, the eccentricity e and the inclination i of the planetesimal with respect to a fictitious body moving with circular velocity

$$V_c = (GM/R)^{1/2} \simeq (GM/l)^{1/2}, \qquad (z \lesssim l/3), \tag{11.4}$$

can be expressed in terms of their relative velocity U with respect to this body (Öpik, 1951; Wetherill, 1967) as

$$GM/a = V_c^2 - 2U_\varphi V_c - U^2, \tag{11.5}$$

$$e^2 = (2U_\varphi/V_c + U^2/V_c^2)^2 + U_R^2(1/V_c^2 - 2U_\varphi/V_c^{3/2} - U^2/V_c^2), \tag{11.6}$$

$$\sin^2 i = U_\zeta^2/(U_\zeta^2 + (V_c + U_\varphi)^2); \tag{11.7}$$

U_R, U_φ, U_ζ are the components of the relative velocity U: $U^2 = U_R^2 + U_\varphi^2 + U_\zeta^2$. We shall use frequently the approximation of echipartition of the components of U with respect to the equatorial plane of the protoplanetary cloud

$$U_R^2 = U_\varphi^2 = U_\zeta^2 = \bar{U}^2/3, \tag{11.8}$$

where $\bar{U}$ denotes the equipartition velocity. For the accretion of the planets $e \lesssim 0.3$ is a sufficient delimitation, so that $\bar{U}$ is generally much smaller than V_c (Figure 10). The

mean values from Equations (11.5)–(11.7) are ($\bar{U}_R = \bar{U}_\varphi = \bar{U}_\zeta = 0$; $U_R^2 = U_\varphi^2 = U_\zeta^2 = \bar{U}^2/3$; Öpik, 1966b)

$$1/a = (V_c^2 - \bar{U}^2)/GM, \tag{11.9}$$

$$e^2 = 5\bar{U}^2/3V_c^2, \qquad e \simeq 5^{1/2}\bar{U}/3^{1/2}V_c, \tag{11.10}$$

$$\sin^2 i = \bar{U}^2/3V_c^2, \qquad \sin i \simeq i \simeq \bar{U}/3^{1/2}V_c. \tag{11.11}$$

We determine subsequently very approximately the change of the relative velocity U in two simple cases:

(A) Change of the relative velocity U due to encounters between planetesimals of equal mass moving in eccentric orbits ($m_1 = m_2 = m$). Let us denote by m_1 and m_2 ($m_1 = m_2 = m$) the masses of two encountering planetesimals with semimajor axes a_1 and a_2 ($a_1 \approx a_2 \approx a$) and with small and equal eccentricities e_1, e_2 ($e_1 = e_2 = e$) and inclinations i_1, i_2 ($i_1 = i_2 = i$) with respect to the equatorial plane of the protoplanetary cloud. U_G denotes the relative velocity of the barycentre of two encountering planetesimals with respect to a circular Keplerian velocity V_c at the point of closest approach, U_1 and U_2 the relative velocities of the two planetesimals with respect to V_c, and U_{G1}, U_{G2} ($U_{G1} = U_{G2}$) the relative velocities of the planetesimals with respect to their barycentre. If $\pi - \xi_1$ denotes the angle between U_G and U_{G1} we have (Figures 4 and 5)

$$U_1^2 = U_G^2 + U_{G1}^2 - 2U_G U_{G1} \cos \xi_1, \tag{11.12}$$

$$U_2^2 = U_G^2 + U_{G2}^2 + 2U_G U_{G2} \cos \xi_1. \tag{11.13}$$

After an encounter U_{G1}, U_{G2} are deflected by an angle γ, which is generally small ($\gamma \ll 1$, see Equation (13.6)), so that U_1, U_2, ξ_1 change by the small quantities ΔU_1, ΔU_2, $\Delta \xi_1$. We get by differentiation of Equations (11.12) and (11.13) and from the spherical triangles in Figure 5 ($U_G = $ const., $U_{G1} = U_{G2} = $ const., $\gamma \ll 1$; cf. Horedt, 1972a, b)

$$U_1 \Delta U_1 = -U_G U_{G1} \Delta \cos \xi_1 \simeq \gamma \sin \xi_1 \cos \eta = -U_2 \Delta U_2, \tag{11.14}$$

because

$$\cos(\pi - \xi_1') = \cos \gamma \cos(\pi - \xi_1) + \sin \gamma \sin(\pi - \xi_1) \cos \eta,$$

and for $\gamma \ll 1$

$$\Delta \cos \xi_1 = \cos \xi_1 - \cos \xi_1' \simeq \gamma \sin \xi_1 \cos \eta.$$

The prime denotes the value of ξ_1 after the encounter.

If V_1, V_2 and V_G denote the velocities of m_1, m_2 and of the barycentre with respect to the Sun, we have from Figure 4

$$V_1^2 = V_G^2 + U_{G1}^2 - 2V_G U_{G1} \cos \nu_1, \tag{11.15}$$

$$V_2^2 = V_G^2 + U_{G2}^2 + 2V_G U_{G2} \cos \nu_1; \tag{11.16}$$
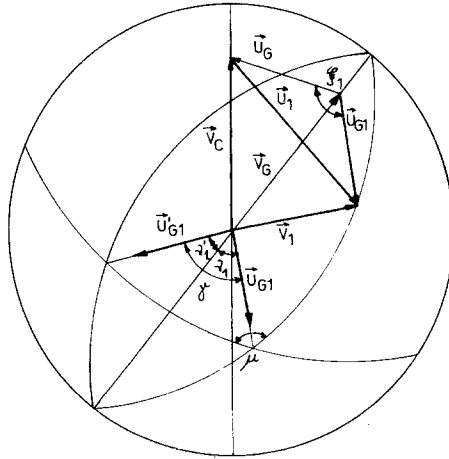
and

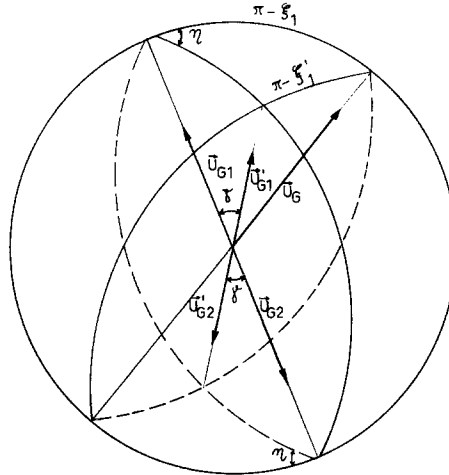Fig. 4.   Gravitational deflection of the velocity vectors ($r_2 \leqslant r \leqslant r_3$).

Fig. 5.   Gravitational deflection of the velocity vectors ($r_2 \leqslant r \leqslant r_3$).

$$V_1 \Delta V_1 = -U_{G1} V_G \Delta \cos \nu_1 \simeq U_{G1} V_G \gamma \sin \nu_1 \cos \mu$$

$$= -V_2 \Delta V_2 = GM \Delta a_1 / 2a_1^2 = -GM \Delta a_2 / 2a_2^2, \qquad (11.17)$$

because

$$\cos (\pi - \nu_1') = \cos \gamma \cos (\pi - \nu_1) + \sin \gamma \sin (\pi - \nu_1) \cos \mu,$$

$$\Delta \cos \nu_1 = \cos \nu_1 - \cos \nu_1' \simeq \gamma \sin \nu_1 \cos \mu, \qquad (\gamma \ll 1),$$

and

$$V_1^2 = GM(2/R - 1/a_1), \qquad V_2^2 = GM(2/R - 1/a_2), \qquad R = \text{const.}$$

We have determined the relative velocity U_{12} between the planetesimals m_1, m_2 in terms of their relative velocity U with respect to a fictitious circularly moving mass point

in the equatorial plane of the protoplanetary cloud. We have (Öpik, 1951)

$$U^2 = 3GM/R - GM/a - 2GMa^{1/2}(1 - e^2)^{1/2} \cos i/R^{3/2}, \tag{11.18}$$

where i is the inclination with respect to the equatorial plane of the protoplanetary cloud. For small eccentricities and inclinations of m we can expand the radius vector as

$$1/R = (1 + e \cos \varphi)/a(1 - e^2) \simeq (1 + e \cos \varphi + e^2)/a,$$

where φ is the anomaly of the elliptic motion. The expression for U becomes

$$U^2 = GM(e^2 - 3e^2 \cos^2 \varphi/4 + i^2 + O(e^3, i^4))/a \simeq GM(5e^2/8 + i^2)/a, \tag{11.19}$$

where we have substituted $\cos^2 \varphi$ by its average value $1/2$. Using Equations (11.10) and (11.11) we find the transformation coefficient between the equipartition velocity $\bar{U}$ and U from Equation (11.19)

$$U^2 \approx GM(25/24 + 1/3)\bar{U}^2/V_c^2 a \approx 11\bar{U}^2/8, \quad U \approx 1.17\bar{U}, \tag{11.20}$$

because for moderate eccentricities $V_c^2 = GM/R \approx GM/a$ up to the first order in e.

The angle i_{12} between the orbits of m_1 and m_2 is related to the inclinations i_1, i_2 of m_1, m_2 with respect to the equatorial plane of the protoplanetary cloud by (Wetherill, 1967; Equation (26))

$$\cos i_{12} = \cos i_1 \cos i_2 + \sin i_1 \sin i_2 \cos \omega_{12}; \tag{11.21}$$

ω_{12} is the angle between the nodes of m_1, m_2 with respect to the equatorial plane. The influence of the last term in Equation (11.21) vanishes on the average, so that $(i_1, i_2 \ll 1)$

$$i_{12}^2 \approx i_1^2 + i_2^2 \quad \text{or} \quad i_{12} \approx 2^{1/2}i, \qquad (i_1 = i_2 = i). \tag{11.22}$$

The direction of the circular velocity V_c' relative to which U_1 and U_2 are defined at the point of encounter is chosen along the bisector of the angle i_{12}, so that

$$U_1^2 = GM(5e_1^2/8 + i_{12}^2/4)/a_1, \quad U_2^2 = GM(5e_2^2/8 + i_{12}^2/4)/a_2, \tag{11.23}$$

where i from Equation (11.20) turns into $i_{12}/2$.

It should be noted that e and i are mean values, the eccentricity and inclination of a planetesimal changing in fact between 0 and a certain maximum value $e_{\max}$, $i_{\max}$, respectively. Therefore, the angle x between U_1 and U_2 changes between 0 and π so that the $\cos x$ term in

$$U_{12}^2 = U_1^2 + U_2^2 - 2U_1 U_2 \cos x \approx U_1^2 + U_2^2 \tag{11.24}$$

vanishes on the average. According to our assumptions $e_1 = e_2 = e$, $i_1 = i_2 = i$, $a_1 \approx a_2 \approx a$, and we find with Equations (11.20), (11.22)–(11.24)

$$U_{12}^2 \approx 2U_1^2 \approx 2GM(5e^2/8 + i_{12}^2/4)/a$$

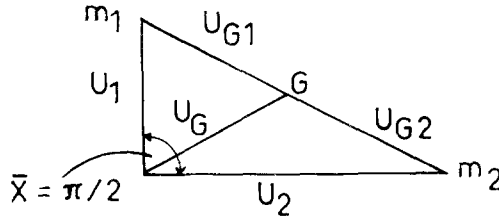$$= 2GM(5e^2/8 + i^2/2)/a \approx 29\bar{U}^2/12 \approx (58/33)U^2. \tag{11.25}$$

Fig. 6.   Average position of the relative velocities.

Equation (11.25) defines a mean approximate relation among: (i) the relative velocity U_{12} between planetesimals moving in orbits of eccentricity e and inclination i with respect to the equatorial plane of the protoplanetary cloud, ($e, i \ll 1$). (ii) the relative velocity U_1 or U_2 ($U_1 \approx U_2$) of the planetesimals with respect to a circular velocity V_c' of inclination $i_{12}/2 = i/2^{1/2} = i_1/2^{1/2} = i_2/2^{1/2}$ relative to the orbits of the planetesimals. (iii) the relative velocity U of the planetesimals with respect to the circular velocity Vc in the equatorial plane of the protoplanetary cloud and (iv) the equipartition velocity $\bar{U}/3^{1/2} = |U_R| = |U_\varphi| = |U_\zeta|$ with respect to the equatorial plane of the protoplanetary cloud.

The transformation coefficients between U_1, U and $\bar{U}$ are close to unity as should be expected on general grounds, but we have preserved them in our calculations

$$U \approx (33/29)^{1/2} U_1 \approx (11/8)^{1/2} \bar{U} \approx (33/58)^{1/2} U_{12}. \qquad (11.26)$$

Because $m_1 = m_2$, we have

$$U_{G1} = U_{G2} = U_{12}/2; \qquad (11.27)$$

and because the mean value $\bar{x}$ of the angle x between the two velocities is close to $\pi/2$ we find from the rectangular triangle of Figure 6 that

$$U_G \approx U_{G1} = U_{G2} = U_{12}/2. \qquad (11.28)$$

The relative velocity U_1 of m_1 with respect to the circular velocity $V_c' = (GM/R)^{1/2}$ can be written according to Equation (11.18), $(i \to i_{12}/2)$

$$U_1^2 = 3GM/R - GM/a_1 - 2GMa_1^{1/2}(1 - e_1^2)^{1/2} \cos (i_{12}/2)/R^{3/2}. \qquad (11.29)$$

At another point of the orbit of m_1 having the radius vector R' the relative velocity can be written as $(|R - R'| \leqslant 2a_1 e_1)$

$$U_1'^2 = 3GM/R' - GM/a_1 - 2GMa_1^{1/2}(1 - e_1^2)^{1/2} \cos (i_{12}/2)/R'^{3/2}. \qquad (11.30)$$

During an encounter between m_1 and m_2 at radius vector R the orbital elements change by $\Delta a_1, \Delta e_1, \Delta i_1$ so that the corresponding change of U_1 is ($R = $ const.)

$$2R^{3/2}U_1\Delta U_1/GM = R^{3/2}\Delta a_1/a_1^2 - \Delta(2a_1^{1/2}(1 - e_1^2)^{1/2} \cos (i_{12}/2)). \qquad (11.31)$$

Due to the change of the orbital elements at radius vector R, the relative velocity U_1' of m_1 at radius vector R' changes as (see Equation (11.30), $R' = $ const.)

$$2R'^{3/2}U_1\Delta U_1/GM = R'^{3/2}\Delta a_1/a_1^2 - \Delta(2a_1^{1/2}(1 - e_1^2)^{1/2} \cos (i_{12}/2)). \qquad (11.32)$$

Combining Equations (11.31) and (11.32) we get the change of the relative velocity

U'_1 at radius vector R' due to a close encounter at radius vector R in the form

$$U'_1 \Delta U'_1 \simeq 3GM(R' - R)\Delta \bar{a}_1 / 4R'a_1^2 + R^{3/2} U_1 \Delta U_1 / R'^{3/2}. \tag{11.33}$$

The mean value of $|R' - R|$ is given by

$$|R' - R| = \int \int_0^{2ae} |R' - R| \, dR' \, dR \Big/ \int \int_0^{2ae} dR' \, dR = 2ae/3. \tag{11.34}$$

With the aid of Equations (11.14), (11.17) and (11.34) the Equation (11.33) turns into

$$U'_1 \Delta U'_1 \approx \pm (a_1 e_1 / R') U_{G1} V_G \gamma \sin \nu_1 \cos \mu + U_G U_{G1} \gamma \sin \xi_1 \cos \eta. \tag{11.35}$$

Taking into account that

$$V_G = (m_1 V_1 + m_2 V_2)/(m_1 + m_2) = (V_1 + V_2)/2,$$
$$V_1 \approx V_2 \approx V_c \quad V_G = V_c + O(ae);$$

Equation (11.35) becomes with Equation (11.10) and for $R' \approx a_1$

$$U'_1 \Delta U'_1 \approx (\pm (5/3)^{1/2} \bar{U} U_{G1} \sin \nu_1 \cos \mu + U_G U_{G1} \sin \xi_1 \cos \eta) \gamma. \tag{11.36}$$

The mean value of the $\sin \nu_1$ averaged over the surface of a sphere of unit radius is

$$\overline{\sin \nu_1} = 2\pi \int_0^\pi \sin^2 \nu_1 \, d\nu_1 / 4\pi = \pi/4 = \overline{\sin \xi_1}; \tag{11.37}$$

and the mean value of $|\cos \mu|$, $|\cos \eta|$

$$\overline{|\cos \eta|} = \overline{|\cos \mu|} = 2/\pi. \tag{11.38}$$

The deflection angle γ is given by (Horedt 1972b, and Equation (13.5))

$$\mathrm{tg}(\gamma/2) \simeq \gamma/2 = G(m_1 + m_2)/U_{12}^2 s, \quad (\gamma \ll 1), \tag{11.39}$$

where s is the target radius of encounter, equal to the distance between m_1 and the asymptote of the hyperbolic orbit of m_2 around m_1. Using Equations (11.37)–(11.39) and the approximate equations (11.27) and (11.28) we finally find that

$$U'_1 \Delta U'_1 \approx [\pm (20/29)^{1/2} \pm 1/2] \gamma U_{12}^2 \approx \pm (20/29)^{1/2} Gm/s \approx -U'_2 \Delta U'_2. \tag{11.40}$$

We have preserved only the larger constant $(20/29)^{1/2}$ because the signs in the rectangular parenthesis of Equation (11.40) can be combined arbitrarily.

(B) Change of the relative velocity due to encounters between a large mass m_p and small planetesimals of mass m $(m_2 = m_p \gg m_1 = m)$. The eccentricity e_p and inclination i_p of the large mass m_p are assumed to be given by the limiting value due to collisions with small planetesimals of mass m with orbits of moderate eccentricity e and inclination i (see Equation (15.14))

$$e_p = e(m/2m_p)^{1/2} \ll e; \quad i_p = i(m/2m_p)^{1/2} \ll i; \tag{11.41}$$

i_p and i being defined with respect to the equatorial plane of the protoplanetary cloud. The semimajor axes of m_p and m are equal up to the first order in e: $a_p = a + O(ae)$.

The relative velocity U_p of m_p with respect to the circular velocity V_c in the equatorial plane is approximately equal to the relative velocity U_G of the barycentre of m_p and m ($m \ll m_p$; (see Equation (11.19))

$$U_G^2 \simeq U_p^2 = GM\,(5e_p^2/8 + i_p^2)/a_p. \tag{11.42}$$

The relative velocity U of m with respect to the circular velocity in the equatorial plane is given by Equation (11.19). From Equations (11.41) and (11.42) we have

$$U_G^2 = GM\,(5me^2/16m_p + i^2m/2m_p) = mU^2/2m_p. \tag{11.43}$$

The relative velocity U_{Gm} between the barycentre and m is approximately equal to the relative velocity U since $U_G \simeq U_p \ll U$: i.e.,

$$U_{Gm} \simeq U. \tag{11.44}$$

The variation of the relative velocity U of m is, according to Equation (11.33),

$$U'\Delta U' = 3GM\,(R' - R)\Delta a/4R'a^2 + R^{3/2}U\Delta U/R'^{3/2}. \tag{11.45}$$

We have, analogously to Equation (11.14),

$$U\Delta U = U_G U_{Gm}\gamma \sin \xi \cos \eta, \tag{11.46}$$

where

$$\gamma \simeq 2Gm_p/U_{Gm}^2 s \simeq 2Gm_p/U^2 s, \quad (\gamma \ll 1). \tag{11.47}$$

Using Equations (11.37)–(11.39), (11.43), (11.44) we obtain

$$U\Delta U = \pm (mm_p)^{1/2}G/2^{1/2}s. \tag{11.48}$$

We have also analogous to Equation (11.17)

$$GM\Delta a/2a^2 = U_G V_G \gamma \sin \nu \cos \mu. \tag{11.49}$$

We discuss the following two cases:

(i) Change of U with respect to the small planetesimals of mass m. In this case, $|R - R'| \approx 2ae/3$ and Equation (11.45) becomes with Equations (11.48) and (11.49) analogous to Equation (11.40), ($e = (40/33)^{1/2}U/V_c$, $V_G \simeq V_c$)

$$U'\Delta U' \approx \pm (40/33)^{1/2}Gm_p/s \pm (mm_p)^{1/2}G/2^{1/2}s \approx (40/33)^{1/2}Gm_p/s. \tag{11.50}$$

(ii) Change of U with respect to the large planetesimal of mass m_p. In this case, $|R - R'| \approx 2a_p e_p/3$ and Equation (11.45) becomes with Equations (11.46) and (11.47)

$$U'\Delta U' \approx \pm e_p U_{Gm} V_G \gamma \sin \nu \cos \mu \pm U_G Gm_p/Us. \tag{11.51}$$

By introducing $e_p = (5/3)^{1/2}\bar{U}_p/V_c = (40/33)^{1/2}U_p/V_c \simeq (40/33)^{1/2}U_G/V_c$ we get

$$U'\Delta U' \approx (\pm (40/33)^{1/2} \pm 1)Gm_p U_G/Us \approx \pm (40/33)^{1/2}Gm_p U_G/Us, \quad (11.52)$$

where $\bar{U}_p$ denotes the equipartition velocity of m_p and we have neglected ± 1 with respect to the larger coefficient $(40/33)^{1/2}$.

12. Principal Equations for the Late Stages of Accretion

The probability of encounter within the maximum target radius for encounters s_g from Equation (11.2) has been determined already by Öpik (1951) and Wetherill (1967). The probability given by Wetherill for eccentric orbits of m_1 and m_2 is of the form

$$p'_e = s_g^2 U_{12}R/8\pi^2 \sin i_{12} |\text{ctg } \alpha_1| a_1^2 a_2^2 (1 - e_1^2)^{1/2}(1 - e_2^2)^{1/2}, \quad (12.1)$$

where

$$\text{ctg } \alpha_1 = U_{1R}R/(GMa_1(1 - e_1^2))^{1/2}. \quad (12.2)$$

U_{1R} denotes the projection of U_1 on the R-axis. The maximum probability of encounter p_e could be four times larger than p'_e, since for four particular values of the perihelion there are possible encounters between m_1 and m_2.

For moderate inclinations we have according to Equations (11.7) and (11.22) $\sin i_{12} \simeq 2^{1/2}U_\zeta/V_c$. $|U_{1R}|$ from Equation (12.2) is independent of the inclination of the orbit and on the average equal to the projection of U on the R-axis $|U_R|$. The average of the product $\sin i_{12}|\text{ctg}\alpha_1| \propto |U_R U_\zeta|$ appearing in the denominator of Equation (12.1) can be estimated as follows: The components of the relative velocity U can be written in terms of the elongation α and of the azimuth β with respect to the φ-direction in the equatorial plane (cf. Öpik, 1966a) as

$$U_R = U \sin \alpha \sin \beta, \quad U_\varphi = U \cos \alpha, \quad U_\zeta = U \sin \alpha \cos \beta. \quad (12.3)$$

The average value of $|U_R U_\zeta|$ over a sphere of unit radius is

$$|U_R U_\zeta| = \int\int_0^{\pi/2} U^2 \sin^3\alpha \sin \beta \cos \beta \, d\alpha d\beta \Big/ \int\int_0^{\pi/2} \sin \alpha \, d\alpha d\beta = 2\bar{U}^2/3\pi, \quad (12.4)$$

where, because of symmetry, we have integrated only over the interval $(0, \pi/2)$. With our assumption of equipartition U turns into $\bar{U}$, which is independent of α and β. The averages of the squared components of U are equal, and we quote as an example only

$$U_R^2 = \int\int_0^{\pi/2} U^2 \sin^3\alpha \sin^2\beta \, d\alpha d\beta \Big/ \int\int_0^{\pi/2} \sin \alpha \, d\alpha d\beta = \bar{U}^2/3,$$

$$U_R^2 = U_\varphi^2 = U_\zeta^2, \quad (12.5)$$

in accordance with Equation (11.8). With Equation (12.4), Equation (12.1) becomes

$$p_e \approx 4p'_e = 3s_g^2 U_{12}G^{1/2}M^{1/2}V_c U_{12}/2^{5/2}\pi\bar{U}^2 a_1^{3/2} a_2^2 (1 - e_2^2)^{1/2}. \quad (12.6)$$

For moderate eccentricities we can neglect e_2^2 and because $\bar{U}^2 = 12U_{12}^2/29$ we find with $a_1 \approx a_2 \approx R$, $V_c = (GM/R)^{1/2}$

$$p_e \approx 29s_g^2 GM/2^{9/2}\pi R^4 U_{12} = (29 \times 33)^{1/2}s_g^2 GM/32\pi R^4 U, \ (z \lesssim l/3).$$

$$(12.7)$$

For a large number of encountering planetesimals and for moderate eccentricities, p'_e from Equation (12.1) takes a value close to its maximum value for circular orbits, i.e, $p_e = 4p'_e$, (Wetherill, 1967).

For the encounter probability of a circularly moving mass m_p with a mass m, Öpik (1951) gives

$$p_{ep} = s_g^2 U/2\pi^2 \sin i|ctg \ \alpha|Ra^2(1-e^2)^{1/2},$$

$$(12.8)$$

which can be transformed analogously to Equation (12.7) into

$$p_{ep} = 33s_g^2 GM/32\pi R^4 U \ (z \lesssim l/3).$$

$$(12.9)$$

As is obvious from Equations (12.7) and (12.9), the quantities p_e and p_{ep} differ only by the factor $(33/29)^{1/2} = 1.07$. We have made calculations for the two cases (A) and (B) already discussed in the previous section.

Case (A): All planetesimals are assumed to have the same mass, eccentricity and inclination.

Case (B): A single major planet of mass m_p moves in an approximately circular orbit encountering planetesimals of much smaller mass m $(m \ll m_p)$, which are assumed to have equal mass, eccentricity and inclination.

As suggested by the numerical work of Dodd and Napier (1974) the second case is much more realistic, but our results for the two cases are for most planets comparable. After n close encounters the expectation of the relative velocity U is, according to Equation (11.1)

$$U^2 = \sum_{k=1}^{n} (\Delta U'_k)^2 = \sum_{k=1}^{n} p_{ek}(\Delta U'_k)^2 \ \Delta t_k,$$

$$(12.10)$$

where p_{ek} is the probability of encounter after the kth encounter and $\Delta t_k = 1/p_{ek}$ the mean interval between encounters. By imparting Δt_k into much smaller steps of length dt we can write Equation (12.10) under the integral form

$$U^2 = \int_0^t p_e \ (\Delta U)^2 dt.$$

$$(12.11)$$

Before introducing Equations (11.40) and (11.50) into Equation (12.11), they should be averaged over s. A mean value of the target radius s can be obtained by observing that the probability $p(s)$ of occurrence of a target radius smaller than s is proportional to the volume of a cylinder of radius s: $p(s) \propto \pi s^2$. The mean value is then (Horedt, 1972a, b)

$$\bar{s} = \int_0^{s_g} s^2 \ ds \bigg/ \int_0^{s_g} s \ ds = 2s_g/3,$$

$$(12.12)$$

because the distribution function of s changes as s when $p(s) \propto s^2$. Introducing Equation (12.12) into Equations (11.40) and (11.50), we obtain

$$\Delta U_1' = \pm (45/29)^{1/2} Gm/U_1' s_g, \tag{12.13}$$

$$\Delta U' = \pm (30/11)^{1/2} Gm_p/U' s_g. \tag{12.14}$$

We discuss separately the two cases from the previous section.

Case (A): Introducing, instead of p_e and ΔU, Equations (12.7) and (12.13) into Equation (12.11), we obtain

$$U_1^2 = \int_0^t 45 G^3 Mm^2 dt/32\pi U_1^3 l^4, (z \lesssim l/3, R \simeq l, U_1' \simeq U_1);$$

and by its differentiation we find that

$$dU_1/dt = 45 G^3 Mm^2/64\pi U_1^4 l^4;$$

or, by taking into account Equation (11.25), we get

or
$$dU_{12}/dt = 45 G^3 Mm^2/2^{7/2} \pi U_{12}^4 l^4$$
$$dU/dt = (33/29)^{5/2} 45 G^3 Mm^2/64\pi U^4 l^4, (z \lesssim l/3). \tag{12.15}$$

Equation (12.15) represents the increase of the velocity dispersion due to mutual encounters between planetesimals of mass m.

Case (B) Introducing Equations (12.9) and (12.14) instead of p_e and ΔU in Equation (12.11) we obtain analogously to Equation (12.15)

$$dU/dt = 45 G^3 Mm_p^2/32\pi l^4 U^4, (z \lesssim l/3). \tag{12.16}$$

Equation (12.16) represents the increase of the velocity dispersion of small planetesimals with equal mass due to encounters with a circularly moving large mass m_p.

The probability of collisions p_c, p_{cp} is obtained if we replace s_g by the target radii for collisions s_c (in Equation (12.7)) for Case (A) between planetesimals of equal mass and by s_{cp} (in Equation (12.9) for Case (B) for collisions between a large planetesimal m_p and small planetesimals of equal mass m. We have

$$p_c = 29 s_c^2 GM/2^{9/2} \pi R^4 U_{12},$$
$$s_c^2 = 4r^2(1 + 8\pi G\delta r^2/3U_{12}^2) = 4(r^2 + 44\pi G\delta r^2/29U^2), \tag{12.17}$$

$$p_{cp} = 33 s_{cp}^2 GM/32\pi R^4 U,$$
$$s_{cp}^2 = (r_p + r)^2 + 8\pi G\delta(r_p^3 + r^3)(r_p + r)/3U^2, \tag{12.18}$$

where r_p and r are, respectively, the radii of m_p and m, and δ is the constant density of the masses m_p and m, ($\delta = 3 \, \mathrm{g\,cm^{-3}}$ for the inner planets, and $\delta = 1.5 \, \mathrm{g\,cm^{-3}}$ for the giant planets and Pluto).

The feeding zone of a planetesimal m_b is approximately equal to the total mass of

the planetesimals having the semimajor axes between $l - el$ and $l + el$:

$$m_b = 2\pi l \sigma_p \Delta l = 4\pi l^2 \sigma_p e, (\Delta l = 2el, z \lesssim l/3), \tag{12.19}$$

where σ_p denotes the total surface density of accretable matter and e is the mean eccentricity of the planetesimals of mass m.

The influence of the gravitational sphere of action s_g to the width of the feeding zone is negligible (see Equations (13.2)–(13.4)).

With Equations (11.10) and (11.25), Equation (12.19) can be expressed in terms of U_{12} (for Case (A)) and U (for Case (B)):

$$m_b = 8 (5/29)^{1/2} \pi l^2 \sigma_p U_{12}/V_c = 8 (10/33)^{1/2} \pi l^2 \sigma_p U/V_c. \tag{12.20}$$

The number N of planetesimals of mass m is for Case (A)

$$N = m_b/m, \tag{12.21}$$

and for Case (B)

$$N = (m_b - m_p)/m. \tag{12.22}$$

During the mean interval $1/p_c$ or $1/p_{cp}$ there occurs one collision of m or m_p with a planetesimal of mass m, so that the growth of the mass m or m_p is given by

$$dm = p_c m \, dt, \tag{12.23}$$

$$dm_p = p_{cp} m \, dt. \tag{12.24}$$

Taking into account that for Case (A) a planetesimal has the chance to collide with $N - 1$ planetesimals of mass m and the large planetesimal m_p (Case (B)) has the chance to collide with N small planetesimals of mass m, the total growth of a planetesimal becomes by using Equations (12.17) and (12.18) and $m_p = 4\pi\delta r_p^3/3$, $m = 4\pi\delta r^3/3$:

Case (A)

$$dr/dt = 29(N - 1)s_c^2 GMm/2^{13/2}\pi^2\delta r^2 l^4 U_{12}, (z \lesssim l/3), \tag{12.25}$$

Case (B)

$$dr_p/dt = 33N s_{cp}^2 GMm/128\pi^2\delta r_p^2 l^4 U, (z \lesssim l/3), \tag{12.26}$$

$$dr/dt = (29 \times 33)^{1/2}(N - 1)s_c^2 GMm/128\pi^2\delta r^2 l^4 U, (z \lesssim l/3). \tag{12.27}$$

According to Equation (12.11) the increase of the velocity dispersion is given for Case (A) by

$$dU_{12}/dt = 45(N - 1)G^3 Mm^2/2^{7/2}\pi U_{12}^4 l^4, (z \lesssim l/3). \tag{12.28}$$

The increase of the velocity dispersion for Case (B) comes from two parts:

(i) From mutual encounters between the small planetesimals of mass m, which is expressed, analogously to Equation (12.28), as

$$(dU/dt)_m = 45 (33/29)^{5/2}G^3 Mm^2/64\pi U^4 l^4. \tag{12.29}$$

(ii) From encounters between the large planetesimal m_p and the small planetesimals

of mass m, which is expressed analogously to Equation (12.16). Because m_p moves in a circular orbit, the relative velocity U between m_p and m remains constant after an encounter. Due to such an encounter there changes only the relative velocity U between the planetesimals of small mass m. Therefore, we have multiplied dU/dt from Equation (12.16) by the additional factor Nm/m_b, taking into account that the relative velocity changes only for the fraction of mass Nm of the mass m_b of the accretion band: i.e.,

$$(dU/dt)_{m_p} = 45G^3MNmm_p^2/32\pi l^4 U^4 m_b. \tag{12.30}$$

The total change dU/dt for Case (B) is given by the sum of Equations (12.29) and (12.30)

$$dU/dt = (dU/dt)_{m_p} + (dU/dt)_m$$
$$= (2Nmm_p^2/m_b + (33/29)^{5/2}(N-1)m^2)45G^3M/64\pi U^4 l^4, \quad (z \lesssim l/3). \tag{12.31}$$

Equation (12.26) for the increase of the radius is, in fact, similar to the usual accretion equation

$$dr_p/dt = s_{cp}^2 U\rho_u/4\delta r_p^2 \tag{12.32}$$

for a mass of radius r_p moving with relative velocity U in a medium of uniform density ρ_u. This can be shown as follows:

The density ρ_u can be expressed by the mass m_b of the accretion band as

$$m_b - m_p = 4\pi l\rho_u z\Delta l = 2\rho_u z m_b/\sigma_p$$

or

$$\rho_u = \sigma_p(1 - m_p/m_b)/2z, \tag{12.33}$$

where z is the height above the equatorial plane of the protoplanetary cloud up to which the uniform medium extends. From Equation (11.11) we have

$$\text{tg } i \simeq i \simeq z/l \simeq \bar{U}/3^{1/2}V_c. \tag{12.34}$$

Introducing z from Equation (12.34) into Equation (12.33), we obtain

$$\rho_u = 3^{1/2}G^{1/2}M^{1/2}\sigma_p(1 - m_p/m_b)/2\bar{U}l^{3/2} \tag{12.35}$$

and

$$dr_p/dt = 3^{1/2}G^{1/2}M^{1/2}s_{cp}^2\sigma_p(1 - m_p/m_b)U/8\delta l^{3/2}r_p^2\bar{U}. \tag{12.36}$$

On the other hand, we get with Equation (12.20) and (12.22)

$$N = m_b(1 - m_p/m_b)/m = 4(5/3)^{1/2}\pi l^{5/2}\sigma_p\bar{U}(1 - m_p/m_b)/G^{1/2}M^{1/2}m; \tag{12.37}$$

and introducing into Equation (12.26) we finally obtain

$$dr_p/dt = 15^{1/2}s_{cp}^2\sigma_p(1 - m_p/m_b)G^{1/2}M^{1/2}U/4\pi\delta r_p^2\bar{U}l^{3/2}. \tag{12.38}$$

Comparing Equation (12.36) to Equation (12.38), which are transformations of Equations (12.32) and (12.26), respectively, we see that they distinguish only by the factor

$$2 \times 5^{1/2}/\pi = 1.42. \tag{12.39}$$

In view of our gross approximations this seems to be a satisfactory agreement.

13. Analytical Solutions

(1) Case A. The relevant equations are (12.25) and (12.28). In a first approximation $8\pi\delta Gr^2/3U_{12}^2$ can be taken as the leading term of the factor s_c^2 from Equation (12.25). With this approximation, the division of Equations (12.25) and (12.28) yields

$$dU_{12}/dr = 45\pi\delta Gr/29U_{12}$$

which integrates to (cf. Safronov, 1969)

$$U_{12} = (45\pi\delta G/29)^{1/2}r. \tag{13.1}$$

With this analytical approximation we can show that the radius of the gravitational sphere of influence s_g is negligible with respect to the width Δl of the accretion band, i.e.

$$s_g = l(m/2M)^{1/3} \ll \Delta l/2 = el = (5/3)^{1/2}\bar{U}l/V_c \tag{13.2}$$

Taking into account Equation (13.1) and $\bar{U} = (12/29)^{1/2}U_{12}, m = 4\pi\delta r^3/3$ we obtain

$$1 \ll 2^{2/3} \times 3^{4/3} \times 5\pi^{1/6}\delta^{1/6}l^{1/2}/29M^{1/6}. \tag{13.3}$$

Indeed, for $l = l_{\text{Mercury}} = 0.4\,\text{AU}$ we have in accordance to Equation (13.3)

$$el/s_g = 1.2 \times 10^2. \tag{13.4}$$

We can show also the consistency of our assumption $\gamma \ll 1$ in Equation (11.39)

$$\gamma = 4Gm/U_{12}^2s \ll 1. \tag{13.5}$$

Taking into account that the mean value of s is $2s_g/3 = 2^{2/3}l(m/M)^{1/3}/3$ we find with Equation (13.1) that

$$\gamma = 3^{1/3} \times 2^{2/3} \times 29M^{1/3}/5\pi^{1/3}\delta^{1/3}l \ll 1, \tag{13.6}$$

if $z \lesssim l/3$ and $l \geqslant 0.4\,\text{AU}$. From Equation (13.1) we obtain

$$8\pi\delta Gr^2/3U_{12}^2 = 232/135 = 1.72, \tag{13.7}$$

so that $8\pi\delta Gr^2/3U_{12}^2$ indeed proves to be the leading term of s_c^2 from Equation (12.25). With Equation (13.7), Equation (12.25) becomes

$$dr/dt = 29 (1 + 232/135)(N - 1)GMm/2^{9/2}\pi^2\delta l^4U_{12}; \tag{13.8}$$

and with Equations (12.20), (12.21) and (13.1) after an elementary integration

TABLE V

Maximum mass $m_{\text{max}} = 4\pi\delta r_{\text{max}}^3/3$ from Equations (13.10) and
(13.13), and the ejection time intervals t_{ej} from Equation (13.18)

Planet	m_{max} [g]	t_{ej} [yr]
Mercury	7.80×10^{26}	2.31×10^{11}
Venus	1.97×10^{27}	2.69×10^9
Earth	3.26×10^{27}	2.92×10^9
Mars	6.11×10^{27}	4.70×10^{11}
Asteroids	1.52×10^{28}	5.40×10^{16}
Jupiter	3.67×10^{29}	3.42×10^5
Saturn	7.84×10^{29}	9.38×10^6
Uranus	2.27×10^{30}	1.14×10^9
Neptune	4.61×10^{30}	1.62×10^9
Pluto	6.67×10^{30}	7.18×10^{13}

$$t = (810\pi^{5/4}\delta^{3/4}l^{11/4}/29 \times 367G^{1/2}\sigma_p^{1/2}M^{3/4}) \ln (r_{\text{max}} + r)/(r_{\text{max}} - r)),$$

where

$$r < r_{\text{max}}, \tag{13.9}$$

$$r_{\text{max}} = (90\sigma_p/29)^{1/2}(\pi l^5/\delta M)^{1/4} \tag{13.10}$$

is the maximum radius attainable by the planetesimals (see Equation (13.13) and Table V). If $r \ll r_{\text{max}}$, Equation (13.9) takes the simple form

$$r = 29^{1/2} \times 367\sigma_p G^{1/2}M^{1/2}t/2^{3/2} \times 5^{1/2} \times 3^3\pi\delta l^{3/2}. \tag{13.11}$$

We have used the approximate initial conditions r, $U_{12} = 0$ if $t = 0$. Equations (13.1) and (13.9) represent the approximate solution for Case (A) and we show that only the surface density σ_p is not known accurately.

The maximum radius r_{max} of a planetesimal can be obtained easily from the condition that the number of planetesimals in the accretion band should be at least $1:N \geqslant 1$. With Equations (12.20) and (12.21) this condition yields

$$N = 8 (5/29GM)^{1/2}\pi\sigma_p l^{5/2}U_{12}/m \geqslant 1, \tag{13.12}$$

or

$$r \leqslant (90 \sigma_p/29)^{1/2}(\pi l^5/M\delta)^{1/4} = r_{\text{max}}. \tag{13.13}$$

As long as $|dl/dt|$ from Equation (10.2) is larger than U_{12} from Equation (13.1) the evolution of planetesimals is characterized by the relative velocity $|dl/dt|$ and occurs according to Section 10. On the other hand, if $U_{12} > |dl/dt|$, the characteristic relative velocity is U_{12} from Equation (13.1) and the evolution occurs according to Section 12.

The separation radius r_2 is obtained by equating Equation (10.2) to Equation (13.1)

$$|dl/dt| = U_{12}, \tag{13.14}$$

or

$$2(l^3/GM)^{1/2}\bar{\rho}W(V_c - V_g)/r_2\delta = (45\pi\delta G/29)^{1/2}r_2;$$

which yields

$$r_2 = 2^{1/2} \times 29^{1/4} l^{3/4} (\bar{\rho} W (V_c - V_g))^{1/2} / 3^{1/2} \times 5^{1/4} \pi^{1/4} \delta^{3/4} G^{1/2} M^{1/4}. \quad (13.15)$$

The separation velocity $|dl/dt|_2 = U_{12}^{(2)}$ from the penultimate column of Table IV is obtained by introducing $r = r_2$ into Equation (10.2) or (13.1).

(2) Case (B). We have obtained analytical solutions for Case (B) only when $m_p \gg Nm$ and when the gravitational interaction between the small planetesimals of mass m is negligible.

(i) Circularly moving planet in a medium of uniform density. An elementary solution can be obtained in terms of Equation (12.32) when the mass m_p moves in a circular orbit around the Sun through a medium of uniform density ρ_u. The relative velocity U remains constant and $s_{cp} \simeq$ const., because m_p is assumed much larger than the mass of accreted dust. The density of accretable matter changes as

$$\rho_u = \rho_{u0} (m_b - m_p) / (m_b - m_{p0}), \quad (13.16)$$

where ρ_{u0} is the density if $m_p = m_{p0}$, $(m_p, m_{p0} \simeq m_b)$. Integrating Equation (12.32) with Equation (13.16) and the initial condition $m_p = m_{p0}$ if $t = 0$, we get a similar equation as Equation (13.9), $(s_{cp}, U = $ const.)

$$t = \ln((m_b - m_{p0})/(m_b - m_p))/\pi s_{cp}^2 m_b \rho_{u0} U, \quad (m_p \gg Nm). \quad (13.17)$$

(ii) Elliptically moving planet. Neglecting the interaction between the small planetesimals of mass m, we can apply Equation (11.52) for the gravitational interaction between the small planetesimals and a much larger planetesimal of mass m_p eccentricity e_p and inclination i_p with respect to the equatorial plane of the protoplanetary cloud. The increase of the relative velocity U occurs according to the quadratic sum rule

$$U^2 = \sum_{k=1}^{n} (p_{ep})_k (\Delta U)^2 \Delta t_k = \int_0^t 45 G^3 M m_p^2 U_G^2 \ dt / 16 \pi l^4 U^5.$$

Taking into account also Equation (11.42), we find analogously to Equation (12.15)

$$dU/dt = 45 G^4 M^2 m_p^2 (5 e_p^2 / 8 + i_p^2) / 32 \pi l^5 U^6;$$

and by integration with the initial conditions $U = 0$ if $t = 0$

$$U^7 = 315 G^4 M^2 m_p^2 (5 e_p^2 / 8 + i_p^2) t / 32 \pi l^5. \quad (13.18)$$

The time interval $t = t_{ej}$ from Equation (13.18) which is needed to increase the relative velocity U up to $U = (2^{1/2} - 1) V_c$ (the ejection limit) is shown in Table V for the actual masses of the planets and for an average eccentricity and inclination e_p, $i_p = 0.05$. Our values for the Earth and Jupiter are $t_{ej} = 1.03 \times 10^{10}$ and 7.08×10^5 yr, respectively, in comparison to 10^9 yr for the Earth ($e_p = 0.02$; $i_p = 0.03$) and 1.5×10^5 yr for Jupiter ($e_p = 0.05$; $i_p = 0.02$) from Öpik's (1966a) Tables 7 and 8. Our results are given in closed form, whereas Öpiks results follow only from his Tables. The disagreement between Equation (13.18) and Öpik's results seems explainable if we take
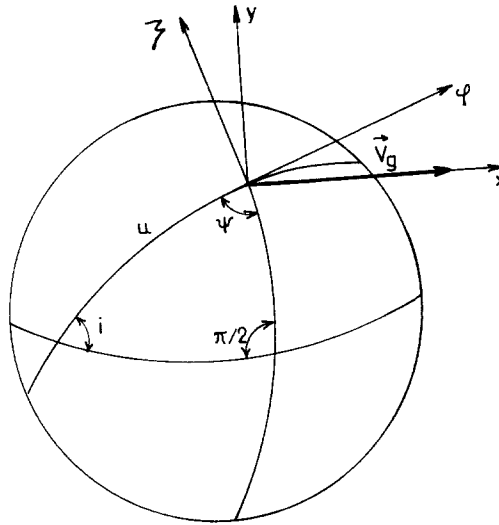
Fig. 7.   Rectangular coordinates for the determination of the effect of gas drag (R, φ, ζ)
and of collisions (R, x, y).

into account the different derivations and the fact that Öpik's (1966a) encounter prob-
abilities are up to two times larger due to his more sophisticated averaging procedure of
p_e, p_{ep}.

It should be noted that Equation (13.18) becomes very uncertain if $U > 0.5V_c$ because
we have assumed for its deduction that $e, i \ll 1$.

14. Effect of Gas Drag

The effect of gas drag on the motion of planetesimals has been investigated recently by
Adachi *et al.* (1976), Weidenschilling (1977a), Donnison and Williams (1977). Generally,
the problem is tractable only numerically (Horedt, 1971, 1973c) but for the case of
small eccentricities and inclinations we deduce simple equations based on the change of
a, e, i for a planetesimal of mass m due to the resistance of the gas

$$da/dt = 2a^{3/2}(-e \sin \varphi P_{iR}/m - pP_{i\varphi}/Rm)/(GM(1 - e^2))^{1/2}, \qquad (14.1)$$

$$de/dt = -(p/GM)^{1/2} \sin \varphi P_{iR}/m - (p/GM)^{1/2}(p/R - R/a)P_{i\varphi}/em, \quad (14.2)$$

$$di/dt = -R \cos u P_{i\zeta}/(GMp)^{1/2}m; \qquad (14.3)$$

where P_{iR}, $P_{i\varphi}$, $P_{i\zeta}$ are the components of the resistance P_i $(i = 1, 2, 3)$ from Equation
(8.10) on the axes from Figure 7: R is the direction of the radius vector from the Sun,
φ is in the orbital plane perpendicular to R and ζ perpendicular to the orbital plane. φ
denotes the anomaly, u the angle between planetesimal and node and $p = a(1 - e^2)$.

If V denotes the Keplerian velocity of the planetesimal, then the relative velocity between planetesimal and gas is

$$v = V - V_g. \tag{14.4}$$

The components of V_g are $V_{gR} = 0$, $V_{g\varphi} = V_g \sin \psi$, $V_{g\zeta} = -V_g \cos \psi$. The φ, ζ, x, y-axes are in the tangential plane of the sphere from Figure 7. The angle $\pi/2 - \psi$ between the φ-axes and V_g is also in the tangential plane. The components of v become (Figure 7)

$$v_R = (GM/p)^{1/2}e \sin \varphi, \quad v_\varphi = (GMp)^{1/2}/R - V_g \sin \psi, \quad v_\zeta = V_g \cos \psi. \tag{14.5}$$

From the spherical triangle in Figure 7 we get

$$\sin \psi = \cos i/(1 - \sin^2 i \sin^2 u)^{1/2} \simeq 1 - i^2 \cos^2 u/2,$$

$$\cos \psi = \sin i \cos u/(1 - \sin^2 i \sin^2 u)^{1/2} \simeq i \cos u, \quad (z \lesssim l/3), \tag{14.6}$$

$$\overline{\sin \psi} = 1 - i^2/4, \quad \overline{\cos \psi} = 0.$$

With $P_i = P_i v/v$ and Equations (14.5) and (14.6), Equation (14.1) becomes

$$\mathrm{d}a/\mathrm{d}t = 2a^{3/2}P_i[-(GM/a)^{1/2}e^2 \sin^2\varphi - (1 + e^2/2)(1 + e \cos \varphi) \times$$

$$\times ((GM/a)^{1/2}(1 + e \cos \varphi)/(1 - e^2)^{1/2}$$

$$- V_g + V_g i^2 \cos^2 u/2)]/(GM)^{1/2}mv + \mathrm{O}(e^3, i^3). \tag{14.7}$$

The term $(1 + e^2/2)$ comes from the expansion of $(1 - e^2)^{-1/2}$ in Equation (14.1). We have substituted also $R = p/(1 + e \cos \varphi)$. After some algebra, Equation (14.7) becomes

$$\mathrm{d}a/\mathrm{d}t = 2a^{3/2}P_i[-(GM/a)^{1/2} + V_g + e \cos \varphi(-2(GM/a)^{1/2} + V_g) +$$

$$+ (GM/a)^{1/2}(-e^2 \sin^2\varphi - e^2 \cos^2\varphi - e^2/2 -$$

$$- i^2 \cos^2 u/2)]/(GM)^{1/2}mv + \mathrm{O}(e^3, i^3). \tag{14.8}$$

Before averaging this equation with respect to the time we have to introduce instead of the anomaly φ the mean anomaly χ, which is a uniform function of time

$$\varphi \simeq \chi + 2e \sin \chi, \quad \cos \varphi \simeq \cos \chi - 2e \sin^2\chi. \tag{14.9}$$

The last term of Equation (14.9) introduces an additional secular term. If we take into account that $\overline{\sin^2\varphi} = \overline{\cos^2\varphi} = \overline{\sin^2\chi} = \frac{1}{2}$ we obtain with Equations (11.10) and (11.11) the average decrease of a equal to

$$\mathrm{d}a/\mathrm{d}t = -2a^{3/2}P_i[(GM/a)^{1/2} - V_g + 11 \bar{U}^2/12(GM/a)^{1/2}]/(GM)^{1/2}mv.$$

If $z \lesssim l/3$ the semi-major axis a is approximately equal to the l-coordinate from the Sun, so that $(V_c \approx (GM/a)^{1/2} \approx (GM/l)^{1/2}, \bar{U}^2 = 8U^2/11)$

$$\mathrm{d}l/\mathrm{d}t = -2l^{3/2}P_i(V_c - V_g + 2U^2/3V_c)/(GM)^{1/2}mv, \quad (z \lesssim l/3). \tag{14.10}$$

For Equation (14.2) we have with Equations (14.5) and (14.6)

$$de/dt = P_i[-e\sin^2\varphi - (p^{3/2}/R^{3/2} - p^{1/2}R^{1/2}/a) \times$$
$$\times ((1 + e\cos\varphi)^{1/2} - V_g(R/GM)^{1/2})/e]/mv + O(i^2). \qquad (14.11)$$

Since $R^{-3/2} \simeq a^{-3/2}(1 + 3e\cos\varphi/2)$ we obtain after some algebra

$$de/dt = P_i[-e\sin^2\varphi - 2\cos\varphi ((GM/a)^{1/2} - V_g) \times$$
$$\times (-1 + e\cos\varphi/2)/V_g]/mv + O(e^2, i^2). \qquad (14.12)$$

Because $(GM/a)^{1/2} - V_g \ll V_g$ the contribution of $2e\sin^2\chi$ from Equation (14.9) is negligible for averaging and we get

$$de/dt = -P_i e/2mv. \qquad (14.13)$$

For the inclination we have from Equation (14.3) with Equations (14.5) and (14.6) the expression

$$di/dt = P_i V_g R\cos u\cos\psi/(GMp)^{1/2}mv = -P_i i\cos^2 u/mv + O(i^2),$$

and for the average decrease of the inclination

$$di/dt = -P_i i/2mv. \qquad (14.14)$$

The average change dU/dt of the relative velocity U due to the gas drag can be easily determined from Equations (14.13) and (14.14). Differentiating Equations (11.10) and (11.11) we have

$$(d\bar{U})_e = (3/5)^{1/2}V_c\, de, \quad (d\bar{U})_i = 3^{1/2}V_c\, di, \qquad (14.15)$$

where $(d\bar{U})_e$, $(d\bar{U})_i$ denotes the variation of the relative velocity due to the variations of e and i, respectively. Because of the smallness of $(d\bar{U})_e$ and $(d\bar{U})_i$ the total change of the relative velocity is given by

$$d\bar{U}/dt = (d\bar{U}/dt)_e + (d\bar{U}/dt)_i = V_c((3/5)^{1/2}\, de/dt + 3^{1/2}\, di/dt). \qquad (14.16)$$

Introducing Equations (14.13) and (14.14) into Equation (14.16) we obtain, with Equations (11.10) and (11.11), $(dU/U = d\bar{U}/\bar{U})$

$$dU/dt = -P_i U/mv. \qquad (14.17)$$

The relative velocity between a planetesimal and the gas could be determined from Equation (14.5) but also by a simple reasoning: The relative velocity of the gas with respect to a fictitious mass moving parallel to the gas with circular velocity V_c is $V_g - V_c$, and the relative velocity between this fictitious mass and a planetesimal is $\approx U$ if $z \lesssim l/3$. According to the simple vector sum rule we have

$$v^2 = U^2 + (V_g - V_c)^2 - 2(V_g - V_c)U\cos\alpha, \qquad (14.18)$$

where α denotes the angle between $V_g - V_c$ and U. By averaging, the $\cos\alpha$ term drops and we get

$$v \approx (U^2 + (V_c - V_g)^2)^{1/2}, \tag{14.19}$$

which is used in our numerical examples.

15. Effect of Collisions

We consider only completely inelastic collisions (e.g., Ziglina and Safronov, 1976), because at the low relative velocities U, U_{12} (Fig. 10) they seem to prevail. Let m_1 and m_2 will be the masses and V_1, V_2 the Keplerian velocities of two colliding planetesimals. Their mass after collision is denoted by m_3, $(m_3 = m_1 + m_2)$, and their velocity follows from the conservation of momentum

$$m_3 V_3 = m_1 V_1 + m_2 V_2. \tag{15.1}$$

(i) Collisions between orbits of low eccentricity and inclination. The components of the velocity V_k $(k = 1, 2, 3)$ on the radial R-direction and on the φ-direction perpendicular to R in the orbital plane are

$$V_{kR} = (GM/a_k(1 - e_k^2))^{1/2}e_k \sin \varphi_k, \;\; V_{k\varphi} = (GMa_k(1 - e_k^2))^{1/2}/R$$
$$(k = 1, 2, 3), \tag{15.2}$$

where a_k, e_k, i_k denote the semi-major axes, the eccentricities and inclinations of m_k. We project $V_{k\varphi}$ on the x, y-axes from Figure 7 in the plane perpendicular to the R-direction: i.e.,

$$V_{kx} = V_{k\varphi} \sin \psi_k, \;\; V_{ky} = V_{k\varphi} \cos \psi_k. \tag{15.3}$$

The projections of Equation (15.1) on the R, x, y-axes are therefore

$$m_1(a_1(1 - e_1^2))^{1/2} \sin \psi_1/R + m_2(a_2(1 - e_2^2))^{1/2} \sin \psi_2/R$$
$$= (m_1 + m_2)(a_3(1 - e_3^2))^{1/2} \sin \psi_3/R, \tag{15.4}$$

$$m_1(a_1(1 - e_1^2))^{1/2} \cos \psi_1/R + m_2(a_2(1 - e_2^2))^{1/2} \cos \psi_2/R$$
$$= (m_1 + m_2)(a_3(1 - e_3^2))^{1/2} \cos \psi_3/R, \tag{15.5}$$

$$m_1 e_1 \sin \varphi_1/(a_1(1 - e_1^2))^{1/2} + m_2 e_2 \sin \varphi_2/(a_2(1 - e_2^2))^{1/2}$$
$$= (m_1 + m_2)e_3 \sin \varphi_3/(a_3(1 - e_3^2))^{1/2}. \tag{15.6}$$

With $\sin \psi_k \approx 1$ from Equation (14.6) we obtain from Equation (15.4)

$$m_1 a_1^{1/2} + m_2 a_2^{1/2} = (m_1 + m_2)a_3^{1/2} + O(e_k^2, i_k^2). \tag{15.7}$$

This latter equation shows that the semi-major axis of two inelastically-colliding particles lies between the two initial semi-major axes and the formation of jet streams as suggested by Alfvén and Arrhenius (1970) is not possible in a medium of very large extensions.

If we use

$$1/R^{1/2} = (1 + e_k \cos \varphi_k)^{1/2}/(a_k(1 - e_k^2))^{1/2}$$

in Equations (15.4) and (15.5) and also the approximation from Equation (14.6), we obtain

$$m_1 e_1 \cos \varphi_1 + m_2 e_2 \cos \varphi_2 = (m_1 + m_2)e_3 \cos \varphi_3 + O(e_k^2, i_k^2),$$

$$m_1 e_1 \sin \varphi_1 + m_2 e_2 \sin \varphi_2 = (m_1 + m_2)e_3 \sin \varphi_3 + O(e_k^2, i_k^2), \qquad (15.8)$$

$$m_1 i_1 \cos u_1 + m_2 i_2 \cos u_2 = (m_1 + m_2)i_3 \cos u_3 + O(e_k^2, i_k^2).$$

If we average the squares of Equations (15.8), the terms $\sin \varphi_1 \sin \varphi_2$, $\cos \varphi_1 \cos \varphi_2$, and $\cos u_1 \cos u_2$, disappear so that

$$(m_1 + m_2)^2 e_3^2 = m_1^2 e_1^2 + m_2^2 e_2^2, \qquad (15.9)$$

$$(m_1 + m_2)^2 i_3^2 = m_1^2 i_1^2 + m_2^2 i_2^2. \qquad (15.10)$$

If $m_1 = m_2 = m$, $e_1 = e_2 = e$, $i_1 = i_2 = i$ we get

$$a_1^{1/2} + a_2^{1/2} = 2 a_3^{1/2}, \quad e_3 = e/2^{1/2}, \quad i_3 = i/2^{1/2}; \qquad (15.11)$$

i.e. after each collision the eccentricity and inclination diminishes by the factor 1.41; whereas the behaviour of the semi-major axes is of no interest, because the extension of the protoplanetary cloud is practically infinite. If $m_2 \gg m_1$, we obtain from Equations (15.7), (15.9), and (15.10)

$$a_3 = a_2 + m_1(a_1 - a_2)/m_2,$$

$$e_3 = e_2 + m_1(m_1 e_1^2 - 2m_2 e_2^2)/2m_2^2 e_2, \qquad (15.12)$$

$$i_3 = i_2 + m_1(m_1 i_1^2 - 2m_2 i_2^2)/2m_2^2 i_2.$$

If $e_2, i_2 \approx 0$, we have

$$e_3 = m_1 e_1/m_2, \quad i_3 = m_1 i_1/m_2. \qquad (15.13)$$

The condition for increase of the eccentricity (inclination) by collisions is from Equation (15.12)

$$\begin{aligned} e_3 > e_2 \quad \text{if} \quad e_2 < e_1 \, (m_1/2m_2)^{1/2}, \\ i_3 > i_2 \quad \text{if} \quad i_2 < i_1 \, (m_1/2m_2)^{1/2}; \end{aligned} \qquad (m_2 \gg m_1) \qquad (15.14)$$

i.e. only if the planetesimal of large mass m_2 has a very low eccentricity (inclination) in comparison to the other planetesimal m_1, the eccentricity (inclination) could increase after collision. The limiting eccentricity and inclination which could be obtained by the planetesimal of large mass is given by Equation (11.41) with the notations $m_1 = m$, $e_1 = e$, $i_1 = i$, $m_2 = m_p$, $e_2 = e_p$, $i_2 = i_p$. Because we have from Eqution (15.14) $e_2 = e_p \ll e = e_1$, $i_2 = i_p \ll i = i_1$ the effect of collisions between m and m_p is neglected for our Case (B) from Section 12. The effect of collisions is taken into account only according to Equations (15.11) for planetesimals of equal mass m.

The change of the orbital elements due to collisions is a discontinuous process with respect to the time. However, this change could be averaged over the mean collision time $1/p_c$ by observing that e and i change by $(1 - 2^{-1/2})e$ and $(1 - 2^{-1/2})i$ during $1/p_c$, so that the differential equation giving the change of e and of i by collisions can be written as

$$de/dt = -p_c(1 - 2^{-1/2})e, \quad di/dt = -p_c(1 - 2^{-1/2})i. \tag{15.15}$$

The total change of the relative velocity U due to collisions is the sum of the changes of U due to the variation of e and i

$$dU/dt = (dU/dt)_e + (dU/dt)_i. \tag{15.16}$$

With Equations (11.10), (11.11) and (15.15) Equation (15.16) transforms into

$$d\bar{U}/dt = V_c((3/5)^{1/2}\, de/dt + 3^{1/2}\, di/dt) \tag{15.17}$$

$$= -p_c(1 - 2^{-1/2})V_c((3/5)^{1/2}e + 3^{1/2}i) = -(2 - 2^{1/2})p_c\bar{U},$$

or

$$dU/dt = -(2 - 2^{1/2})p_c U. \tag{15.18}$$

(ii) Collisions between a large planetesimal m_2 and small planetesimals m_1 ($m_2 \gg m_1$). We assume that m_2 has an orbit of moderate eccentricity and inclination, while m_1 has an approximately parabolic velocity. We project Equation (15.1) on the R-axis, so that

$$m_3 V_{3R} = m_1 V_{1R} + m_2 V_{2R}. \tag{15.19}$$

We have ($p_2 = a_2(1 - e_2^2)$, e_2, $i_2 \ll 1$)

$$V_{2R} = (GM/p_2)^{1/2}e_2 \sin \varphi_2$$

$$= V_c e_2 \sin \varphi_2 (1 + e_2 \cos \varphi_2)^{1/2} \simeq e_2 V_c \sin \varphi_2 ;$$

and by averaging over $\cos \varphi_2$

$$V_{2R} = \pm 2e_2 V_c/\pi. \tag{15.20}$$

For the evaluation of the change of inclination we project Equation (15.1) on the y-axis

$$m_3 V_{3y} = m_1 V_{1y} + m_2 V_{2y}, \tag{15.21}$$

and observe that, according to Equations (14.6) and (15.3), we can write

$$V_{2y} = V_{2\varphi} \cos \psi_2 \simeq V_c \sin i_2 \cos u_2 \simeq i_2 V_c \cos u_2 ;$$

and by averaging over $\cos u_2$,

$$V_{2y} = \pm 2i_2 V_c/\pi. \tag{15.22}$$

Assuming equipartition of the velocities V_1 of the parabolically moving small planetesimals, we can write

$$V_{1R} \approx V_{1y} \approx \pm (2GM/R)^{1/2}/3^{1/2} = \pm (2/3)^{1/2} V_c. \tag{15.23}$$

We observe that, in a first approximation, the average values of V_{2R} and V_{2y} are equal if we substitute e_2 for i_2. Therefore, we confine ourselves only to the discussion of Equation (15.19), the final result being equally valid also for Equation (15.21). We have

$$
\begin{aligned}
m_3 V_{3R} &= m_1 V_{1R} + m_2 V_{2R} \\
&= m_1 V_{1R} + (m_3 - m_1) V_{2R} \simeq m_1 V_{1R} + m_3 V_{2R},
\end{aligned} \tag{15.24}
$$

since $m_2 = m_3 - m_1 \simeq m_3, (m_2 \gg m_1)$. Equation (15.24) also states that

$$m_1 V_{1R} \simeq m_3 (V_{3R} - V_{2R}) = m_3 \Delta V_{3R},$$

$$(V_{3R} \simeq V_{2R}, \ \Delta V_{3R} = V_{3R} - V_{2R}). \tag{15.25}$$

The changes ΔV_{3R} from individual collisions accumulate according to a quadratic sum rule. If the initial value of V_{3R} is zero, after n collisions we have

$$V_{3R}^2 = \sum_{k=1}^{n} (\Delta V_{3R})_k^2 = \sum_{k=1}^{n} (m_1 V_{1R}/m_3)_k^2$$

$$= (2V_c^2/3) \sum_{k=1}^{n} (m_1/m_3)_k^2. \tag{15.26}$$

If we make the plausible assumption that the masses m_1 grow together with m_3 in such a way that $m_1/m_3 \approx$ const. during the accretional collisions, (Figure 9), then Equation (15.26) becomes

$$V_{3R}^2 = 2n V_c^2 k_m^2/3, \tag{15.27}$$

where $k_m = m_1/m_3$ denotes the mean value of m_1/m_3 during n successive collisions. Since after each collision $V_{3R} \simeq V_{2R}$, $m_3 \simeq m_2$, $m_1/m_3 \simeq m_1/m_2$, we can use Equation (15.20) to obtain

$$V_{3R}^2 \simeq V_{2R}^2 = 4e_2^2 V_c^2/\pi^2. \tag{15.28}$$

With the notations from our Case (B) $(m_1 = m, m_2 = m_p, m \ll m_p)$ and $e_2 = e_p, i_2 = i_p$ we obtain from Equations (15.27) and (15.28)

$$e_p \approx i_p \simeq \pi(n/6)^{1/2} k_m, \ (k_m = m/m_p). \tag{15.29}$$

The mass increase dm_p of m_p due to dn collisions with small planetesimals of mass m is

$$dm_p = k_m m_p dn \text{ or } n = (1/k_m) \ln (m_p/m_{p0}), \tag{15.30}$$

where m_{p0} is the initial value of m_p for $n = 0$ collisions. With Equation (15.30), Equation (15.29) can be written as
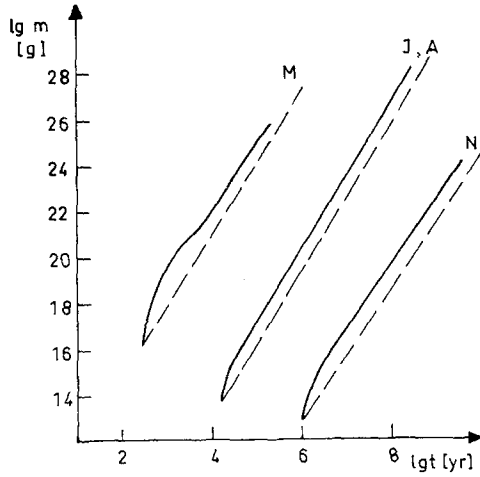
Fig. 8. Case (A) Mass increase of the planetesimals of equal mass. Continuous lines: collisions and gas drag are considered. Broken lines: Analytical solution from Equation (13.9) without the effect of gas drag and collisions; the asymptotic behaviour of r is omitted. The curves labeled with M, A, J, N are for Mercury, the asteroids, Jupiter and Neptune, respectively.
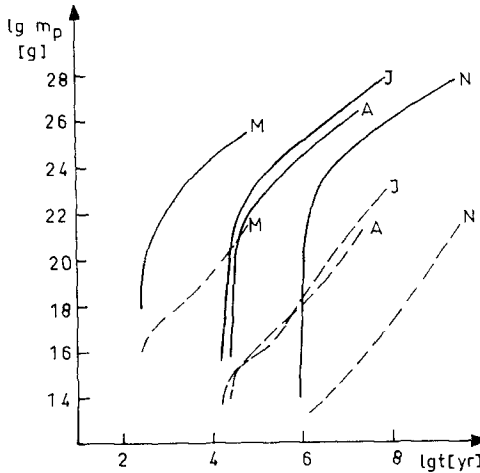

Fig. 9. Case (B) Mass increase of the large planetesimal m_p (continuous lines) and of the small planetesimals of mass m (broken lines) for Mercury (M), the asteroids (A), Jupiter (J) and Neptune (N).

$$e_p = i_p = \pi(k_m \ln(m_p/m_{p0})/6)^{1/2}, \qquad (15.31)$$

where for our calculations from Figures 8 and 9 we have $\ln(m_p/m_{p0}) \lesssim 30$.

If we assume, for instance, in Equation (15.29) $k_m = 10^{-2}$ about 60 collisions with nearly parabolically moving planetesimals are necessary to increase the eccentricity and inclination of the large planetesimal to 0.1, a maximum value for most planets. If $k_m = 10^{-3}$ – a value suggested by Safronov (1969; Table 12) from the inclinations of

planetary spin axes – about 6000 collisions are necessary to produce the same effect; $n = 6000$ if $k_m = 10^{-3}$ yields, from Equation (15.30), $\ln (m_p/m_{p0}) \approx 6$, which is compatible with our limitation $\ln (m_p/m_{p0}) \lesssim 30$. On the other hand, if $m/m_p = 0.08$ there is necessary only a single collision ($n = 1$) to produce an eccentricity or inclination of 0.1.

We conclude that collisions with nearly parabolically moving planetesimals could have contributed substantially to the actual eccentricities and inclinations of the planets, because collisions between planetesimals of moderate eccentricity and inclination are extremely inefficient to produce appreciable increase of the eccentricity and inclination of m_p, according to Equations (15.13) and (15.14). Since no precise values of $k_m = m/m_p$ are available, we have neglected the above-mentioned possibility in our numerical examples.

16. Numerical Results and Conclusions

The equations used for our numerical integrations follow easily from Equations (12.25)–(12.28), (12.31), (14.10), (14.17) and (15.18).

Case (A): Planetesimals of equal mass, eccentricity and inclination. U_{12} is the relative velocity between planetesimals and $z \lesssim l/3$.

$$dr/dt = 29(N - 1)s_c^2 GMm/2^{13/2}\pi^2\delta r^2 l^4 U_{12}, \tag{16.1}$$

$$dU_{12}/dt = 45(N - 1)G^3Mm^2/2^{7/2}\pi U_{12}^4 l^4 - $$
$$- 29s_c^2 GM(N - 1)(1 - 2^{-1/2})/2^{7/2}\pi l^4 - P_i U_{12}/mv, \tag{16.2}$$

$$s_c^2 = 4r^2(1 + 8\pi\delta Gr^2/3U_{12}^2), \tag{16.3}$$

$$v = (33U_{12}^2/58 + (V_c - V_g)^2)^{1/2}, \tag{16.4}$$

$$dl/dt = - 2lP_i(V_c - V_g + 11U_{12}^2/29V_c)/mvV_c. \tag{16.5}$$

Case (B): A major planetesimal of mass m_p orbiting circularly in the equatorial plane of the protoplanetary cloud and numerous small planetesimals of equal mass, eccentricity and inclination. The symbol U stands for the relative velocity between the large and the small planetesimals, and $z \lesssim l/3$. Furthermore,

$$dr_p/dt = 33Ns_{cp}^2 GMm/128\pi^2\delta r_p^2 l^4 U, \tag{16.6}$$

$$dr/dt = (29 \times 33)^{1/2}(N - 1)s_c^2 GMm/128\pi^2\delta r^2 l^4 U, \tag{16.7}$$

$$dU/dt = [2Nmm_p^2/m_b + (33/29)^{5/2}(N - 1)m^2]45G^3M/64\pi U^4 l^4 - $$
$$- (29 \times 33)^{1/2}s_c^2 GM(N - 1)(1 - 2^{-1/2})/16\pi l^4 - P_i U/mv, \tag{16.8}$$

$$s_{cp}^2 = (r_p + r)^2 + 8\pi G\delta(r_p^3 + r^3)(r_p + r)/3U^2, \tag{16.9}$$

$$s_c^2 = 4r^2(1 + 44\pi G\delta r^2/29U^2), \tag{16.10}$$

$$v = (U^2 + (V_c - V_g)^2)^{1/2}, \tag{16.11}$$

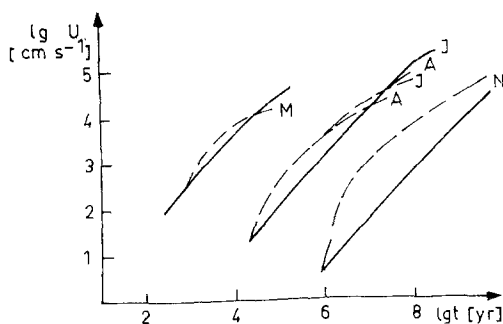$$dl/dt = - 2lP_i(V_c - V_g + 2U^2/3V_c)/mvV_c. \tag{16.12}$$

Fig. 10. The relative velocity U_{12} of the planetesimals from Case (A) (continuous lines) and the relative velocity U of the small planetesimals from Case (B) (broken lines). The analytical solution without gas drag and collisions from Equation (13.1) has approximately the same form as the continuous lines.
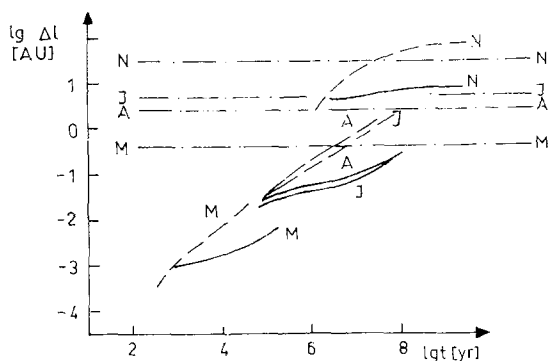

Fig. 11. Decrease of the semi-major axes of the planetesimals from Case (A) (continuous lines) and of the small planetesimals from Case (B) (broken lines). The broken-dotted lines denote the actual semi-major axes of the planets: M — Mercury, A — asteroids, J — Jupiter, N — Neptune.

Dodd and Napier (1974) found from a numerical simulation of the accretion process that there form a few planetesimals of very large mass m_p in comparison to the mean mass m of the majority of the other planetesimals. Therefore we have started the integration for our Case (B) with $m_p/m = 64$. This ratio increases during the integration up to 10^4 (for the terrestrial planets) and up to 10^7 (for the outer planets) as it is obvious from Figure 9.

As suggested by observations, we made the assumption that between the asteroids and Jupiter there occurs a density jump of the surface density σ_p of planetesimals: inside the orbits of the asteroids the planetesimals are formed from the rocky fraction of matter of the protoplanetary cloud (mass fraction 0.00343) and outside from rock and ice (mass fraction 0.0158; cf. Section 6, and Podolak and Cameron, 1974).

It is likely that we have overestimated by the above assumption the density jump by a factor of 1.5, because near the orbit of Jupiter there have condensed probably only
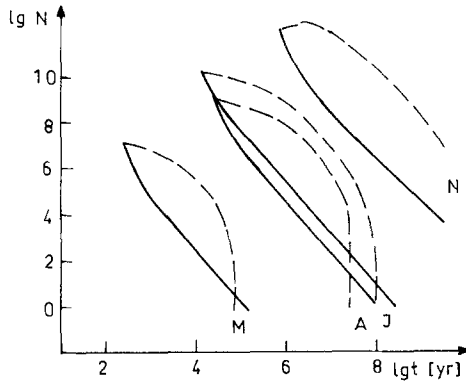
Fig. 12.   Decrease of the number of planetesimals in the accretion zone of Mercury (M), the Asteroids (A), Jupiter (J) and Neptune (N). Continuous lines are for Case (A), broken lines for Case (B).

water (mass fraction 0.00694 condensing at about 170 K) and ammonia (mass fraction 0.00111 condensing at about 140 K; Podolak and Cameron, 1974). The remaining fraction of methane (mass fraction 0.00432, condensing at about 60 K) is likely to condense only at the orbits of Uranus and Neptune, (see our Table I). In view of the other uncertainties we neglect this overestimate and summarize below the principal conclusions:

(i) As a general rule we observe that the accretion time of planetesimals increases by several orders of magnitude from Mercury to Pluto: If $r < r_2$, the accretion time increases from several hundred years for Mercury to several 10^6 yr for Pluto; if $r_2 < r < r_3$ from 10^5–10^9 yr (Tables III, IV, VI; Figures 8 and 9). r_2 comes from Table IV and r_3 is the final radius corresponding to the mass $m_3 = 4\pi\delta r_3^3/3$ from Table VI.

(ii) Because of the jump of the surface density between the asteroids and Jupiter, the planetesimals evolve at nearly the same time scale in both regions, but the final mass is about 30 times larger in the region of Jupiter (Figures 8 and 9, Table IV). This seems to be the cause that Jupiter accreted also gas from the protoplanetary cloud, its mass increasing grossly. The planetesimals accelerated by Jupiter during 10^5–10^6 yr (Table V) accreted and/or destroyed the planetesimals in the region of the asteroids, (e.g., Weidenschilling, 1975). The actual asteroids appear as the remainders of a much larger population. The fact that eccentricities and inclinations are of the same order of magnitude in the asteroid belt ($e \approx i$) favors the assumption that they originated from collisions according to Equation (15.31) and not from close encounters for which we have $e/i = 5^{1/2}$ according to Equations (11.10) and (11.11).

(iii) An unexpected result of our calculations are the low final masses m_3 for the terrestrial planets, ($\approx 10^{26}$ g). Because of the high collision probability in the terrestrial region ($p_c \propto l^{-4}$) the number of planetesimals drops quickly to 1 in an accretion band (Figure 12).

This situation is not changed drastically if we assume the gas drag to be absent, as occurs after blowing away of the gaseous component of the protoplanetary cloud by a

TABLE VI

The mass m_3 which accretes during the interval $t_3 - t_2$ if $r_3 \leqslant r \leqslant r_2$, $m_{3,\text{obs}}$ denotes the actual mass of the planets without H and He. The cases (A) and (B) from columns 3–6 are already explained in the text. Case (B1) is identical to Case (B), but without the effect of gas drag. Case (B2) is identical to Case (B), but instead of the surface density σ from Table II we have put 3σ. After 3×10^9 yr the integration was stopped.

Case		A		B		B1		B2	
Planet	$m_{3,\text{obs}}$ [g]	m_3 [g]	$t_3 - t_2$ [yr]	m_3 [g]	$t_3 - t_2$ [yr]	m_3 [g]	$t_3 - t_2$ [yr]	m_3 [g]	$t_3 - t_2$ [yr]
Mercury	3.30×10^{26}	6.75×10^{25}	1.27×10^{5}	3.30×10^{25}	6.62×10^{4}	3.11×10^{26}	7.40×10^{6}	1.41×10^{26}	2.40×10^{4}
Venus	4.87×10^{27}	1.52×10^{26}	9.85×10^{5}	6.90×10^{25}	3.61×10^{5}	7.94×10^{26}	6.80×10^{7}	2.92×10^{26}	1.54×10^{5}
Earth	5.98×10^{27}	2.35×10^{26}	2.82×10^{6}	1.03×10^{26}	9.66×10^{5}	1.31×10^{27}	2.15×10^{8}	4.33×10^{26}	4.09×10^{5}
Mars	6.42×10^{26}	4.03×10^{26}	1.09×10^{7}	1.67×10^{26}	3.39×10^{6}	2.44×10^{27}	9.42×10^{8}	7.05×10^{26}	1.42×10^{6}
Asteroids	3.00×10^{24}	8.90×10^{26}	7.89×10^{7}	3.47×10^{26}	2.11×10^{7}	5.01×10^{27}	3.00×10^{9}	1.45×10^{27}	8.81×10^{6}
Jupiter	2.50×10^{29}	2.15×10^{28}	2.29×10^{8}	8.92×10^{27}	7.03×10^{7}	9.12×10^{28}	3.00×10^{9}	3.71×10^{28}	2.89×10^{7}
Saturn	1.90×10^{29}	4.99×10^{28}	1.75×10^{9}	1.75×10^{28}	4.37×10^{8}	5.99×10^{28}	3.00×10^{9}	7.28×10^{28}	1.73×10^{8}
Uranus	7.40×10^{28}	5.49×10^{26}	3.00×10^{9}	3.64×10^{28}	3.00×10^{9}	9.78×10^{27}	3.00×10^{9}	1.79×10^{29}	1.49×10^{9}
Neptune	7.70×10^{28}	5.30×10^{24}	3.00×10^{9}	9.23×10^{27}	3.00×10^{9}	2.57×10^{27}	3.00×10^{9}	1.37×10^{29}	3.00×10^{9}
Pluto	6.00×10^{26}	4.31×10^{23}	3.00×10^{9}	4.25×10^{27}	3.00×10^{9}	1.17×10^{27}	3.00×10^{9}	5.55×10^{28}	3.00×10^{9}

T-Tauri-like solar wind (Horedt, 1978a). The masses m_3 of the terrestrial planets obtained by taking into account the effect of collisions and gas drag are considerably lower than the maximum mass m_{max} (Table V), obtained from the analytical solution of Section 13, without regarding collisions and gas drag.

Because of their small mass, the terrestrial planets were probably never surrounded by large atmospheres and did not accrete gas from the protoplanetary cloud. Their small masses seem to be also the principal cause of absence of well developed satellite systems.

(iv) Another unexpected result in accordance with observations are the large masses (10^{28} g) for the non-gaseous component of the giant planets, excepting Uranus and Neptune for Case (A), Figure 8, Table VI. These large masses occur because the relative velocities U_{12} or U increase sufficiently fast to assure the spreading of the accretion band as the planetesimals grow in mass. Because, for Uranus and Neptune, the time of accretion is very long ($p_c \propto l^{-4}$; $t_3 - t_2 \gtrsim 10^9$ yr) these planets cannot accrete an appreciable fraction of the principal gaseous components H and He, since these gases are blown away during 10^8 yr, (see next point).

(v) Spiraling in due to gas drag has been calculated according to Equations (16.5) and (16.12). We have also taken into account the decrease of density with height by assuming that the gas of surface density σ extends only up to the height $z^* = \sigma/\bar{\rho}$. Above z^* the gas drag is zero.

The inward motion of the small planetesimals m in Case (B) would be larger than their distance from the Sun in the region of the outer planets, so that they leave during about 10^8 yr the accretion zone of these planets. The large planetesimals of equal mass m in Case (A) have also considerable inward motion if the gas drag persisted for about 10^8 yr, ($\Delta l \approx 8$ AU for Neptune, Figure 11).

The maximum time during which the gases are blown away from the inner part of the solar system can be estimated as follows: For simplicity, we consider approximately circular orbits. In this case Equations (16.5) and (16.12) become for the resistance law P_3, $(e, i, U \approx 0; v \approx V_c - V_g)$

$$dl/dt = -3\bar{\rho}(V_c - V_g)^2 l/2rV_c\delta$$
and
$$t = 2r\delta V_c(\Delta l/l)/3\bar{\rho}(V_c - V_g)^2. \tag{16.13}$$

Substituting the relevant values for Mercury we find that, for $\Delta l/l = 1/4$, $t = 7.8 \times 10^7$ yr. Thus if the planets are assumed to have formed at their actual distance from the Sun, the gases from the inner part of the protoplanetary cloud should have been blown away during 10^7–10^8 yr (Horedt, 1978a). Otherwise there occurs a considerable decrease of the semi-major axes, even with the most generous assumptions.

From Equation (14.13), it can be shown that the large eccentricity of Mercury arose only when the gas of the protoplanetary cloud was blown away from its zone. When gas drag is present, Equation (14.13) becomes ($P_i = P_3$)

$$de/dt = -\pi\bar{\rho}r^2 v e/2m = -3^{3/2} \times 11^{1/2}e^2 V_c\bar{\rho}/2^{9/2} \times 5^{1/2}r\delta, \tag{16.14}$$

where we have used $v \approx U$ and Equations (11.10) and (11.26). Integration of Equation (16.14) with the initial conditions $e = e_0$ at $t = 0$ yields if $e_0 \gg e$

$$t = 2^{9/2} \times 5^{1/2} r \delta / 3^{3/2} \times 11^{1/2} \bar{\rho} V_c e. \tag{16.15}$$

Introducing the values for Mercury we find that its eccentricity would decrease from e_0 ($e_0 \gg e$) to its actual value $e = 0.2$ during the very short time interval of 6600 yr.

(vi) General Conclusions. In the region of the terrestrial planets there accreted during 10^5–10^7 yr several tens or hundred planetesimals of mass $\approx 10^{26}$ g. The increase of the mass fraction of accretable matter by about 4.5 times between the region of the asteroids and of Jupiter causes the latter to become more massive (Figures 8 and 9; Table VI) and to accrete probably also matter from the region of the asteroids and of Mars.

Without any additional assumptions, Jupiter and Saturn accrete a very large fraction of planetesimals ($\approx 10^{28}$ g), and because of their large mass they would accrete later also the major part of the gas. For Case (B), Uranus and Neptune grow also to appreciable mass but only within several 10^9 yr.

Comets appear to originate from (i) planetesimals ejected by the giant planets (Öpik, 1966a, b; Everhart, 1973; and our Table V); (ii) an original population of planetesimals outside the region of Uranus, where because of the low collision probability a large number of planetesimals could be preserved (see Figure 12).

(vii) The major inconsistency of our model. A comparison between the actual non-gaseous component of the planets $m_{3,\text{obs}}$ from Table VI and our mass values m_3 from Figures 8, 9 and Table VI shows that our model fails to give the correct final masses for most planets by at least one order of magnitude. Excepting Uranus and Neptune this occurs because the number of planetesimals in an accretion band of width $2el$ falls too fast below unity and integration must be stopped.

A first point against our model could be made by questioning the validity of our equations (16.1)–(16.12). If we suppose, for instance, that for a given radius r_p the relative velocity U is larger by several times than in our calculation, the inner planets could grow to their actual masses without difficulty, but the time scales for the formation of the planets outside Jupiter are much too long ($\gg 10^9$ yr). This occurs because of the substantial decrease of the second factor containing U_{12}^{-2}, U^{-2} in Equations (16.3), (16.9) and (16.10). The crucial role of the lowering of U by gas drag and collisions for the formation of the outer planets comes also from this factor.

On the other hand, if U becomes much lower than in our models, the final masses m_3 for the inner planets become even much smaller than in Table VI. A test calculation shows that an increase of the encounter and collision probability p_e, p_{ep}, p_c, p_{cp} by a factor of 2 has merely the effect to decrease the time of formation of the planets by this factor and to increase the final mass (not the radius!) of the planets inside Saturn by the same factor.

We conclude that there is little scope to modify the numerical factors arising from our averaging procedures, though our simple treatment is certainly not very exact for very close encounters, i.e. for large deflection angles.

Fragmentation of colliding planetesimals seems to be not relevant in view of the low relative velocities (Figure 10).

If we increase the poorly known surface density σ of the protoplanetary cloud by three times (see Case (B2) from Table VI), Uranus and Neptune accrete without difficulty during 10^9 yr, whereas the masses of the planets up to Saturn increase only about three times in comparison to Case (B). If we increase artificially the width of the accretion band, the final masses m_3 increase approximately by the same factor, as shown by a test calculation.

We conclude that the sole difficulty of our model is the fact that the accretion band of the planets up to Saturn is devoided too fast from accretable planetesimals. This difficulty could arise in our opinion from two sides, which can hardly be included in our averaged equations (16.1)–(16.12):

(i) In reality there arises a certain dispersion of the orbital elements a, e, i and of the masses. This dispersion could permit a much better argument between $m_{3,\text{obs}}$ and m_3 from Table VI, because planetesimals with very small inclinations are accreted much faster than according to our averaged equations, while planetesimals with very large eccentricities allow for a considerable increase of the width of the accretion band.

(ii) Close encounters are the most efficient perturbations as long as the orbits of planetesimals intersect. When this is no longer the case ($N \leqslant 1$), then secular perturbations of non-intersecting orbits become the sole perturbing factor, which can be efficient as shown by numerical examples (Horedt *et al.*, 1977).

Acknowledgement

References

Adachi, I., Hayashi, C. and Nakazawa, K.: 1976, *Prog. Theor. Phys.* 56, 1756.
Alfvén, H. and Arrhenius, G.: 1970, *Astrophys. Space Sci.* 8, 338; 9, 3.
Anders, E.: 1972, In *L'origine du Système Solaire*, (H. Reeves, ed.), CNRS Paris, p. 179.
Arrhenius, G. and Alfvén, H.: 1971, *Earth Planet. Sci. Lett.* 10, 253.
Arrhenius, G. and Asunmaa, S. K.: 1973, *The Moon* 8, 368.
Bandermann, L. W.: 1972, *Mon. Not. Roy. Astr. Soc.* 160, 321.
Black, D. C. and Bodenheimer, P.: 1976, *Astrophys. J.* 206, 138.
Bodenheimer, P.: 1972, *Rep. Prog. Phys.* 35, 1.
Cameron, A. G. W. and Pine, M. R.: 1973, *Icarus* 18, 377.
Cameron, A. G. W.: 1973, *Icarus* 18, 407.
Chandrasekhar, S.: 1939, *An Introduction to the Study of Stellar Structure*, Univ. of Chicago Press.
Coradini, A., Magni, G. and Federico, C.: 1977, *Astrophys. Space Sci.* 48, 79.
Dodd, R. J. and Napier, W. Mc. D.: 1974, *Astrophys. Space Sci.* 29, 51.
Donnison, J. R. and Williams, I. P.: 1977, *Mon. Not. Roy. Astr. Soc.* 180, 289.
Everhart, E.: 1973, *Astr. J.* 78, 329.
Ferrer, O. and Jaschek, C.: 1973, *Publ. Astr. Soc. Pac.* 85, 207.

Giuli, R. T.: 1968, *Icarus* **9**, 186.
Goldreich, P. and Ward, W. R.: 1973, *Astrophys. J.* **183**, 1051.
Haar, D. ter,: 1972, In *L'origine du Système Solaire*, (H. Reeves, ed.), CNRS Paris, p. 71.
Hallam, M. and Marcus, A. H.: 1974, *Icarus* **21**, 66.
Harris, A. W.: 1977, *Icarus* **31**, 168.
Hartmann, W. K.: 1970, *Mém. Soc. Roy. Liège* **19**, 215.
Horedt, G. P.: 1970, *Mon. Not. Roy. Astr. Soc.* **151**, 81.
Horedt, G. P.: 1971, *Astr. Astrophys.* **14**, 223.
Horedt, G. P.: 1972a, *Acta Astr.* **22**, 55.
Horedt, G. P.: 1972b, *Celest. Mech.* **6**, 232.
Horedt, G. P.: 1973a, *Mon. Not. Roy. Astr. Soc.* **163**, 285.
Horedt, G. P.: 1973b, *Astr. Astrophys.* **23**, 303.
Horedt, G. P.: 1973c, *Astrophys. Space Sci.* **22**, 321.
Horedt, G. P.: 1974a, *Acta Astr.* **24**, 207.
Horedt, G. P.: 1974b, *Icarus* **22**, 230.
Horedt, G. P.: 1974c, *Icarus* **23**, 459.
Horedt, G. P.: 1975a, *Astrophys. Space Sci.* **35**, L15.
Horedt, G. P.: 1975b, *Astr. Astrophys.* **44**, 461.
Horedt, G. P.: 1975c, *Prog. Theor. Phys.* **54**, 1224.
Horedt, G. P.: 1976, *Astrophys. Space Sci.* **45**, 353.
Horedt, G. P., Pop, P., Ruck, H.: 1977, *Celest. Mech.* **16**, 209.
Horedt, G. P.: 1978a, *Astr. Astrophys.* **64**, 173.
Horedt, G. P.: 1978b, *Astrophys. Space Sci.* **54**, 253.
Kaula, W. M. and Bigeleisen, P. E.: 1975, *Icarus* **25**, 18.
Kiladze, R. I.: 1970, *Bull. Abastumani Astrophys. Obs.* **39**, 103.
Kusaka., T, Nakano, T. and Hayashi, C.: 1970, *Prog. Theor. Phys.* **44**, 1580.
Larson, R. B.: 1972a, In *L'origine du Système Solaire*, (H. Reeves, ed.), CNRS Paris, p. 142.
Larson, R. B.: 1972b, *Mon. Not. Roy. Astr. Soc.* **157**, 121.
Lewis, J. S.: 1972, *Earth Planet. Sci. Lett.* **15**, 286.
Lewis, J. S.: 1974, *Science* **186**, 440.
Mestel, L.: 1970, *Mém. Soc. Roy. Sci. Liège* **19**, 167.
Miki, S. and Nakano, T.: 1975, *Publ. Astr. Soc. Japan* **27**, 147.
Mitra, V.: 1970, *Astr. Astrophys.* **4**, 263.
Nieto, M. M.: 1975, *Icarus* **25**, 171.
Okamoto, I.: 1969, *Publ. Astr. Soc. Japan* **21**, 25.
Öpik, E. J.: 1951, *Proc. Roy. Irish Acad.* **54**, 165.
Öpik, E. J.: 1966a, *Mém. Soc. Roy. Sci. Liège* **12**, 523.
Öpik, E. J.: 1966b, *Adv. Astr. Astrophys.* **4**, 301.
Podolak, M. and Cameron, A. G. W.: 1974, *Icarus* **22**, 123.
Safronov, V. S.: 1969, *Evolution of the Protoplanetary Cloud and Formation of the Earth and of the Planets*, Moscow, Nauka Press.
Scalo, J. M.: 1977, *Astr. Astrophys.* **55**, 253.
Weidenschilling, S. J.: 1975, *Icarus* **26**, 361.
Weidenschilling, S. J.: 1977a, *Mon. Not. Roy. Astr. Soc.* **180**, 57.
Weidenschilling, S. J.: 1977b, *Astrophys. Space Sci.* **51**, 153.
Weis, E. W.: 1974, *Astrophys. J.* **190**, 331.
Wetherill, G. W.: 1967, *J. Geophys. Res.* **72**, 2429.
Weizsäcker, C. F. v.: 1943, *Z. Astrophys.* **22**, 319.
Whipple, F. L.: 1972, In *From Plasma to Planet*, (A. Elvius, ed.), Nobel Symp. **21**, 211.
Williams, I. P. and Crampin, D. J.: 1971, *Mon. Not. Roy. Astr. Soc.* **152**, 261.
Ziglina, I. N. and Safronov, V. S.: 1976, *Astr. Zh.* **53**, 429.